

**GENETIC ALGORITHM-BASED DAMAGE CONTROL  
FOR SHIPBOARD POWER SYSTEMS**

A Thesis

by

TUSHAR AMBA

Submitted to the Office of Graduate Studies of  
Texas A&M University  
in partial fulfillment of the requirements for the degree of

MASTER OF SCIENCE

May 2009

Major Subject: Electrical Engineering

**GENETIC ALGORITHM-BASED DAMAGE CONTROL  
FOR SHIPBOARD POWER SYSTEMS**

A Thesis

by

TUSHAR AMBA

Submitted to the Office of Graduate Studies of  
Texas A&M University  
in partial fulfillment of the requirements for the degree of

MASTER OF SCIENCE

Approved by:

|                     |                       |
|---------------------|-----------------------|
| Chair of Committee, | Karen L. Butler-Purry |
| Committee Members,  | Chanan Singh          |
|                     | Shankar Bhattacharyya |
|                     | Sergiy Butenko        |
| Head of Department, | Costas N. Georghiades |

May 2009

Major Subject: Electrical Engineering

## ABSTRACT

Genetic Algorithm-Based Damage Control for Shipboard Power Systems.

(May 2009)

Tushar Amba, B.E., Thapar Institute of Engineering and Technology

Chair of Advisory Committee: Dr. Karen L. Butler-Purry

The work presented in this thesis was concerned with the implementation of a damage control method for U.S. Navy shipboard power systems (SPS). In recent years, the Navy has been seeking an automated damage control and power system management approach for future reconfigurable shipboard power systems. The methodology should be capable of representing the dynamic performance (differential algebraic description), the steady state performance (algebraic description), and the system reconfiguration routines (discrete events) in one comprehensive tool. The damage control approach should also be able to improve survivability, reliability, and security, as well as reduce manning through the automation of the reconfiguration of the SPS network.

To this end, this work implemented a damage control method for a notional Next Generation Integrated Power System. This thesis presents a static implementation of a dynamic formulation of a new damage control method at the DC zonal Integrated Flight Through Power system level. The proposed method used a constrained binary genetic algorithm to find an optimal network configuration. An optimal network configuration is a configuration which restores all of the de-energized loads that are possible to be

restored based on the priority of the load without violating the system operating constraints. System operating limits act as constraints in the static damage control implementation. Off-line studies were conducted using an example power system modeled in PSCAD, an electromagnetic time domain transient simulation environment and study tool, to evaluate the effectiveness of the damage control method in restoring the power system. The simulation results for case studies showed that, in approximately 93% of the cases, the proposed damage algorithm was able to find the optimal network configuration that restores the power system network without violating the power system operating constraints.

To my family and friends

## ACKNOWLEDGEMENTS

I would like to thank my committee chair, Dr. Karen L. Butler-Purry, for the support and encouragement throughout the course of this research. I am grateful to her for providing me an opportunity to work as a research assistant on this project.

I wish to thank my committee members, Dr. Chanan Singh, Dr. Shankar Bhattacharyya, and Dr. Sergiy Butenko, for their guidance and support throughout the course of this research.

Thanks also go to my friends and colleagues and the department faculty and staff for making my time at Texas A&M University a great experience.

Finally, thanks to my family for their love, support and words of encouragement.

## TABLE OF CONTENTS

|  | Page |
|--|------|
| ABSTRACT .....   | iii  |
| DEDICATION .....   | v    |
| ACKNOWLEDGEMENTS .....   | vi   |
| TABLE OF CONTENTS .....  | vii  |
| LIST OF FIGURES.....   | x    |
| LIST OF TABLES .....   | xii  |
| 1. INTRODUCTION.....   | 1    |
| 1.1. Introduction .....  | 1    |
| 1.2. Research Objectives .....   | 2    |
| 1.3. Organization of the Thesis .....  | 3    |
| 2. LITERATURE REVIEW .....   | 4    |
| 2.1. Shipboard Power System .....  | 4    |
| 2.2. Damage Control .....  | 7    |
| 2.3. Genetic Algorithm.....  | 11   |
| 3. PROBLEM FORMULATION .....   | 15   |
| 3.1. Introduction .....  | 15   |
| 3.2. DC Zonal Power System Model.....  | 15   |
| 3.3. Analytical Formulation of Dynamic Damage<br>Control Method for DC Zonal System..... | 18   |
| 3.4. Genetic Algorithm-Based Damage Control Method<br>for DC Zonal System.....           | 23   |
| 3.5. Summary .....   | 23   |
| 4. IMPLEMENTATION DETAILS: GENETIC ALGORITHM-<br>BASED DAMAGE CONTROL METHOD.....        | 24   |
| 4.1. Introduction .....  | 24   |

|   | Page |
|---|------|
| 4.2. Damage Control Algorithm Module .....  | 24   |
| 4.2.1. Genetic Algorithm Sub-Module .....   | 26   |
| 4.2.1.1. Initialization .....   | 28   |
| 4.2.1.2. Repair-and-Replace Process .....   | 32   |
| 4.2.1.3. Objective Function Evaluation .....  | 35   |
| 4.2.1.4. Selection .....  | 38   |
| 4.2.1.5. Recombination .....  | 40   |
| 4.2.1.6. Mutation .....   | 41   |
| 4.2.1.7. Reinsertion .....  | 42   |
| 4.2.1.8. Migration .....  | 43   |
| 4.2.2. DAE Solver and System Operating<br>Constraints Sub-Module .....                  | 44   |
| 4.3. Summary .....  | 45   |
| 5. CASE STUDIES AND SIMULATIONS .....   | 46   |
| 5.1. Introduction .....   | 46   |
| 5.2. Power System Simulation Model .....  | 46   |
| 5.3. Failure Assessment Module and Pre/Post-Fault<br>Information Extractor Module ..... | 50   |
| 5.4. Case Studies .....   | 50   |
| 5.4.1. Case Study 1 .....   | 51   |
| 5.4.1.1. Initial Conditions .....   | 51   |
| 5.4.1.2. Fault Scenario .....   | 52   |
| 5.4.1.3. Simulation Results .....   | 52   |
| 5.4.2. Case Study 2 .....   | 53   |
| 5.4.2.1. Initial Conditions .....   | 54   |
| 5.4.2.2. Fault Scenario .....   | 54   |
| 5.4.2.3. Simulation Results .....   | 54   |
| 5.4.3. Case Study 3 .....   | 55   |
| 5.4.3.1. Initial Conditions .....   | 56   |
| 5.4.3.2. Fault Scenario .....   | 56   |
| 5.4.3.3. Simulation Results .....   | 56   |
| 5.4.4. Case Study 4 .....   | 57   |
| 5.4.4.1. Initial Conditions .....   | 58   |
| 5.4.4.2. Fault Scenario .....   | 58   |
| 5.4.4.3. Simulation Results .....   | 58   |
| 5.4.5. Case Study 5 .....   | 59   |
| 5.4.5.1. Initial Conditions .....   | 60   |
| 5.4.5.2. Fault Scenario .....   | 60   |
| 5.4.5.3. Simulation Results .....   | 61   |
| 5.4.6. Case Study 6 .....   | 61   |

|                                      | Page |
|--------------------------------------|------|
| 5.4.6.1. Initial Conditions.....     | 62   |
| 5.4.6.2. Fault Scenario.....         | 62   |
| 5.4.6.3. Simulation Results.....     | 62   |
| 5.5. Summary of Results .....        | 63   |
| 5.6. Summary .....                   | 65   |
| 6. CONCLUSION .....                  | 66   |
| 6.1. Overview of Research Work ..... | 66   |
| 6.2. Conclusions .....               | 67   |
| 6.3. Future Work .....               | 67   |
| REFERENCES .....                     | 69   |
| VITA .....                           | 72   |

## LIST OF FIGURES

| FIGURE   | Page |
|--|------|
| 2.1 Example AC radial shipboard power system .....                     | 5    |
| 2.2 Notional next generation SPS architecture.....                     | 7    |
| 2.3 Structure of single-population genetic algorithm.....              | 13   |
| 2.4 Structure of multi-population genetic algorithm.....               | 14   |
| 3.1 Notional NGIPS DC zonal IFTP system.....                           | 17   |
| 3.2 Bus transfer switch.....   | 21   |
| 4.1 Problem implementation: block diagram for damage control .....     | 25   |
| 4.2 Genetic algorithm sub-module flow chart.....                       | 27   |
| 4.3 Overall chromosome structure for notional<br>DC zonal system.....  | 29   |
| 4.4 Chromosome structure for one zone: incoming switches .....         | 29   |
| 4.5 Chromosome structure for one zone: non-vital DC load switches..... | 30   |
| 4.6 Chromosome structure for one zone: vital DC load switches.....     | 30   |
| 4.7 Chromosome structure for one zone: non-vital AC load switches..... | 31   |
| 4.8 Chromosome structure for one zone: vital AC load switches.....     | 31   |
| 4.9 Chromosome structure for one zone: outgoing switches .....         | 32   |
| 4.10 Switches not to be closed .....                                   | 33   |
| 4.11 PCM-4 switches .....  | 34   |
| 4.12 Multi-point crossover .....                                       | 41   |
| 4.13 Binary valued mutation .....                                      | 41   |

| FIGURE   | Page |
|--|------|
| 4.14 Elitist reinsertion scheme .....  | 42   |
| 4.15 Unrestricted migration topology .....   | 44   |
| 5.1 Problem implementation: off-line process to<br>test the damage control method..... | 47   |
| 5.2 Problem implementation: example power system .....                                 | 49   |
| 5.3 Overall results of solution category .....   | 64   |

**LIST OF TABLES**

| TABLE  | Page |
|--|------|
| 5.1 Power system example: load details.....  | 48   |
| 5.2 Power system example: cable details..... | 48   |
| 5.3 Results of case study 1 .....            | 53   |
| 5.4 Results of case study 2 .....            | 55   |
| 5.5 Results of case study 3 .....            | 57   |
| 5.6 Results of case study 4 .....            | 59   |
| 5.7 Results of case study 5 .....            | 61   |
| 5.8 Results of case study 6 .....            | 63   |

# 1. INTRODUCTION

## 1.1. Introduction

In recent years, the U.S. Navy has been seeking an automated damage control and power system management approach for future reconfigurable Shipboard Power Systems (SPSs) [1]. The methodology should be capable of representing the dynamic performance (differential algebraic description), the steady state performance (algebraic description), and the system reconfiguration routines (discrete events) in one comprehensive tool [1]. The damage control approach should also be able to improve survivability, reliability, and security, as well as reduce manning through the automation of the reconfiguration of the SPS network.

SPSs are affected by dynamics such as disturbances and faults, which can occur in rapid succession and by external factors such as battle damages. Both may cause disruption of power supply to critical loads resulting in a ship mission failure. Therefore, it is imperative to isolate the faulted section(s) and restore service quickly to as many of the critical loads as possible without violating the power system operating constraints. The restoration of service is achieved through reconfiguration of the SPS network while optimally managing the power system resources.

## 1.2. Research Objectives

The research work presented in this thesis is a part of ongoing research project conducted at Power System Automation Laboratory (PSAL) at Texas A&M University, College Station. Currently, researchers at the Power System Automation Laboratory (PSAL) at Texas A&M University are developing dynamic solutions for various power management functions, including damage control, to implement on Next Generation Integrated Power System (NGIPS) SPS. In one possible solution, the dynamic damage control problem for NGIPS was formulated as constrained optimization problems for implementation at two different levels of the SPS: High/Medium Voltage (HV/MV) AC system and DC zonal Integrated Flight Through Power (IFTP) system. The optimal control problem was constrained by system operating conditions and system dynamics. The objectives of this research study presented in this thesis were:

- a) To implement a damage control method at notional NGIPS DC zonal IFTP system level.
- b) To implement a genetic algorithm-based static approach with penalty functions and heuristic rules to solve the constrained optimization problem for DC zonal IFTP system level using only power system operating limits as constraints.
- c) To perform cases studies to demonstrate various different aspects, load restoration and load shedding, of the proposed method.

### **1.3. Organization of the Thesis**

The thesis is organized into six sections. Section 1 provides the introduction and overall research objectives for the research work conducted at PSAL. Section 2 presents the literature review conducted in the areas of SPS, damage control, and genetic algorithm. Section 3 provides the details of the dynamic damage control problem formulation. Section 4 presents the implementation details of the static damage control method at notional NGIPS DC zonal IFTP system level. Section 5 presents various case studies conducted to demonstrate various different aspects of the solution proposed. Finally Section 6 presents the conclusion for the research work.

## 2. LITERATURE REVIEW

### 2.1. Shipboard Power System

In the past few years the idea of employing a common power system for both propulsion and ship's services has inspired a lot of research in the field of shipboard power system. Current generation of ship utilize Combined Diesel and Diesel (CODAD), Combined Diesel and Gas (CODAG), Combined Gas and Gas (COGAG) or Combined Diesel Electric and Gas (CODLAG) propulsion configuration [2]. Conversion of these systems to complete electric system, not only reduces the fuel cost, but also reduces the size of the propulsion components and their cost.

The current generation of the ship employs AC radial systems for ship's auxiliaries. Propulsion system is not included in the electric power system. Propulsion system is driven with diesel engines. In ac radial shipboard power systems generators [3] are connected in a ring formation through generator switchboards. All these generator switchboards connected through bus-tie circuit breaker, which defines the flow of power. Load centers and few individual loads are fed from generator switchboard. Further power panels are supplied through the load centers. Critical loads are usually are provided with two supply path i.e. normal supply path and alternate supply path. Non-critical loads have a single supply source. In case of a fault or disturbances, to restore the vital loads, non-vital loads are shed, if required. An example AC radial shipboard power system is presented in Fig. 2.1.

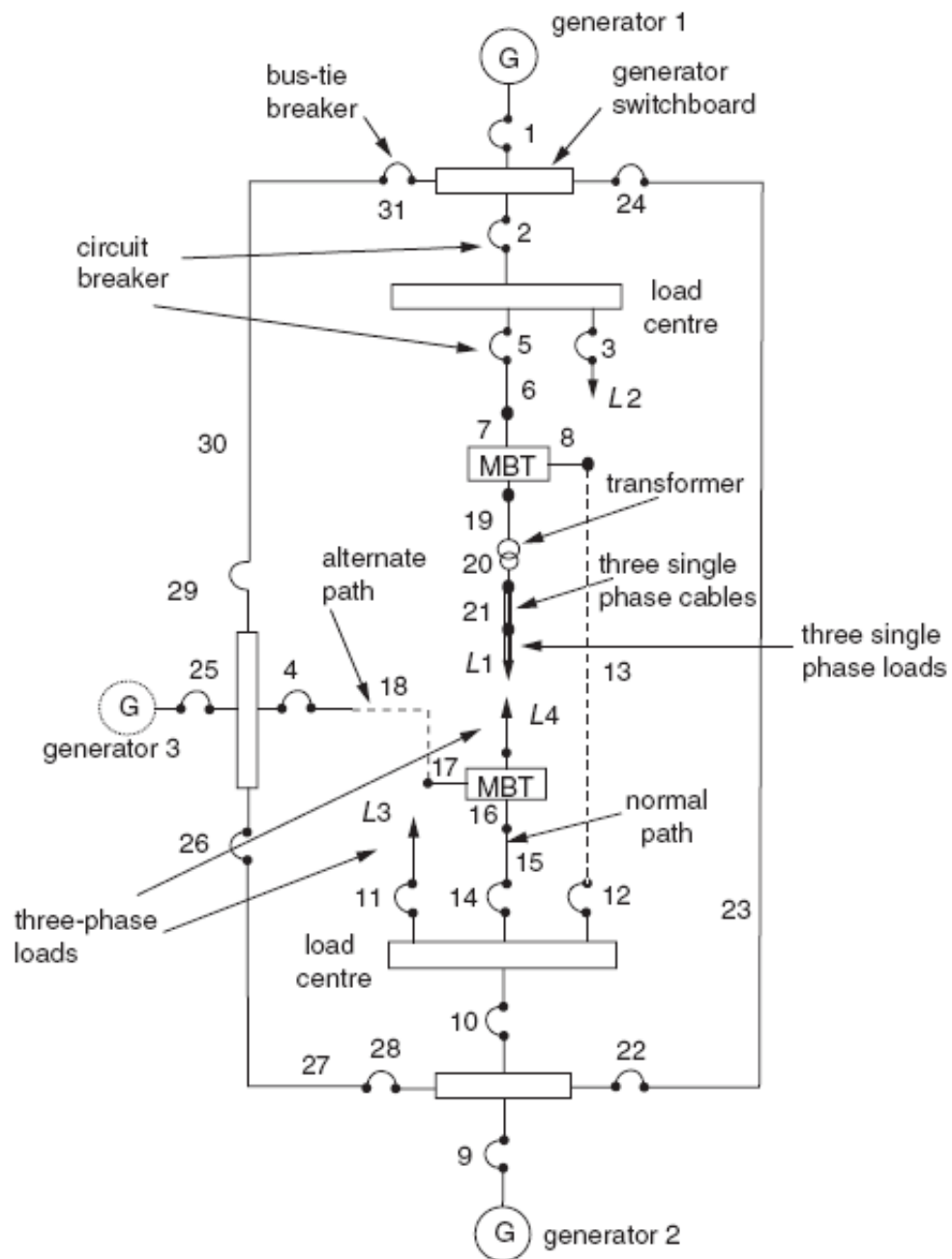


Fig. 2.1. Example AC radial shipboard power system [4]

The Integrated Power System (IPS), a ship architecture in which a common electrical source supplies both ship service loads and ship propulsion, is considered to be the basic architecture for the next generation ship [5]. The research reported in this thesis applies the damage control method to a notional NGIPS model. The notional NGIPS consists of a HV/MV AC system and a DC zonal IFTP system, as shown in Fig. 2.2. The HV/MV AC system consists of four 13.8 kV generators connected in a ring arrangement. The total capacity of the generation system is 80 MW, comprising two main generators, MTG1 and MTG2, with power ratings of 36 MW each, and two auxiliary generators, ATG1 and ATG2, with power ratings of 4 MW each. There are four three-phase step down transformers, which reduces the 13.8 kV bus voltages to the 4.16 kV level. The 4.16 kV system supplies power to the ship propulsion system and the DC zonal system. The Power Conversion Module-4 (PCM-4) converts the 4.16 kV AC system voltage to the 1 kV DC distribution voltage. The notional NGIPS has four PCM-4s, each connected to a DC zone. Each DC zone contains two PCM-1s that convert the 1 kV DC distribution voltage to 375 V DC, 650 V DC, and 800 V DC levels. The 375 V DC and 650 V DC levels are used to supply power to DC loads. The PCM-2s are connected to the 800 V DC nodes and convert 800 V DC to three-phase 450 V AC, which supplies power to the AC loads in the zones. The DC/AC loads in the zones are categorized as either vital (V) or non-vital (NV) loads. While the non-vital loads have only one supply path, the vital loads have two possible supply paths via bus transfers.

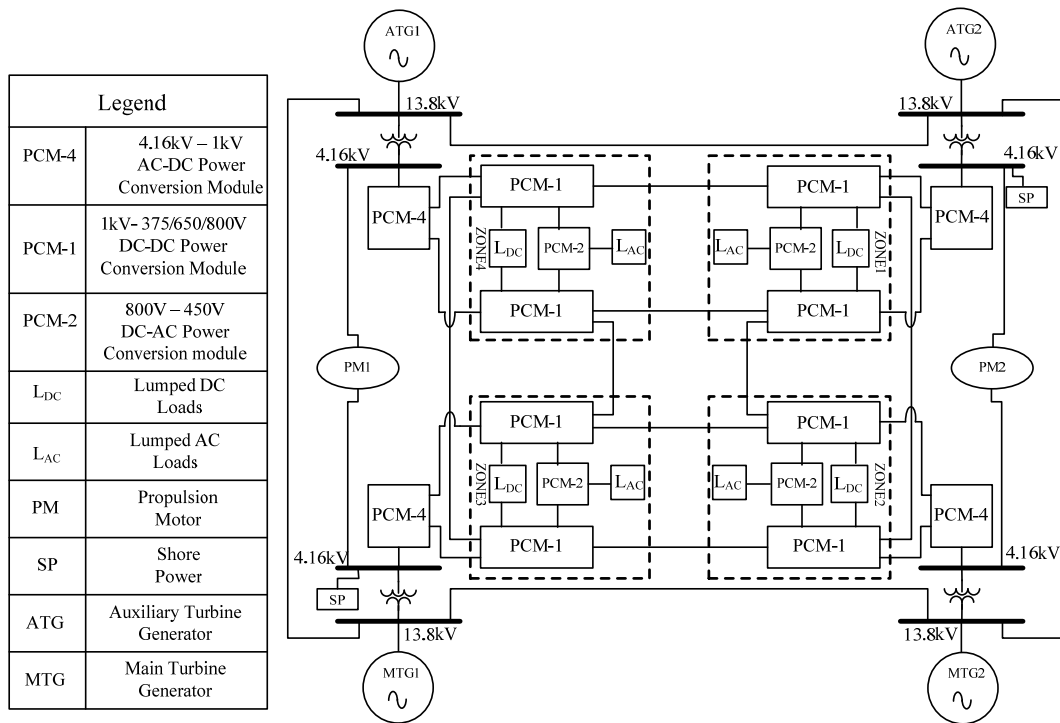


Fig. 2.2. Notional next generation SPS architecture

## 2.2. Damage Control

Distribution automation [6] for SPS has inspired a great deal of interest in the past few years. The idea behind the distribution automation is to improve survivability, security, reduced manning and automated reconfiguration for shipboard power system network. One of the important functionalities under distribution automation is damage control / service restoration. Service restoration is the process of fault isolation, load restoration and load shedding by reconfiguring the power system network without violating the operating constraints.

SPSs are affected by dynamics such as disturbances and faults, which can occur in rapid succession and by external factors such as battle damages. Both may cause

disruption of power supply to critical loads resulting in a ship mission failure. Therefore, it is imperative to isolate the faulted section(s) and restore service quickly to as many of the critical loads as possible without violating the power system operating constraints. The restoration of service is achieved through reconfiguration of the SPS network while optimally managing the power system resources. However, sometimes it is not always possible to restore all the de-energized loads without violating the system constraints; therefore, loads with higher priority are restored first and loads with lesser priority may be shed in order to meet the system constraint.

Though there has been abundant research on the problem of terrestrial power system restoration and shipboard power system damage control, only a few researchers have incorporated the dynamics of the power system into the solution. Most researchers have addressed the restoration/damage control problem with static solutions such as [7]-[13], which perform reconfiguration considering the steady state performance of the power system. The methods which have attempted to incorporate power system dynamics into the service restoration problem are presented in [14]-[16]. The authors in [16] presented a dynamic programming algorithm for hybrid power systems that solves dynamic optimization problems involving both binary (discrete) and real (continuous) variables. Continuous dynamics for power systems were modeled using differential algebraic equations (DAEs) and discrete acting subsystem associated with logical specifications were converted to mixed-integer formulas which define the transition conditions between discrete states of the system [16]. The hybrid control method was illustrated in the thesis using a small example power system [16]. The authors in [14]

presented a reconfiguration approach for SPS which uses a multi-agent system. The problem [14] was formulated as a maximization problem constrained by static power system operating conditions. The authors in [14] illustrated the method using a test SPS. In [15], the authors presented a reconfiguration technique using equivalent dynamic impedance representation of the power system. The problem was formulated as an optimization problem and the equivalent impedances are computed dynamically from real time voltage and current measurements [15].

Also, damage control problem is a NP-complete combinatorial problem, which makes it difficult to solve. However, for this problem there may be many possible solutions, or no solution may exist. This kind of problem requires adequate modeling and analysis of system components, network topology, system flow and constraints to be solved optimally. Various algorithms have been proposed in the past to find solutions for damage control problem. These approaches can be broadly classified as:

- Intelligent and heuristic techniques: genetic algorithm [17]-[20], particle swarm optimization [13], simulated annealing, neural network [11], [12], expert systems [3], [9], fuzzy logic [10] and agent based techniques [14].
- Classical techniques: Mixed integer programming [8], [21].

In [21] a solution technique based on Integer Linear Programming with heuristic rules for distribution feeder reconfiguration for service restoration is presented. The problem is formulated as optimization problem with minimization of switching actions during reconfiguration/load assignment as the objective function. The method presented in [21] is independent of the initial configuration and is efficient and robust. But, in case

the feasible solution does not exist, this method cannot provide a “best possible solution”, which can minimize the inevitable load drop. Also, the use of mixed integer programming restricts the choice of objective function and constraints. In [3] an expert-system based method is presented for automatic reconfiguration of SPS. The method, based on certain heuristic rules, tries to determine the control operation required to restore the de-energized load for the AC radial SPS after battle damage or cascading faults [3]. Though the method is quite fast and efficient, the solution provided by this method may not be optimal.

A reconfiguration methodology, using a genetic algorithm, is presented in [20] that reconfigures a power system network, satisfying the operational requirements and priorities of the load. The problem is formulated as an optimization problem with maximization of the power delivered to the loads as the objective function. The authors used graph theory to convert the power system into graph and then apply genetic algorithm for service restoration. Though a very simple objective function is used, genetic algorithm can be applied irrespective of the objective function and topology making it useful for functions that are highly non-linear. Also, the method presented in [20] is applicable for non-radial system, such as SPS. In another paper [17], an algorithm based on genetic algorithm with simulated annealing is presented for multi-objective service restoration for power distribution system. The purpose of genetic algorithm is to find the Pareto optimal solution set. The algorithm in [17] combines genetic algorithm and simulated annealing to improve the precision of the solutions and also to avoid local optima. The reconfiguration problem in [17] is formulated as a multi-objective problem

with minimizing the total amount of de-energized load and minimizing the number of switching actions as the two objectives. But, the method presented in [17] is limited to radial systems only. Intelligent algorithms such as genetic algorithm, simulated annealing and particle swarm optimization have advantage over other techniques in terms of choice of objective functions and handling a large number of equality and inequality constraints. But, these techniques suffer from the problem of premature convergence.

Approaches such as neural networks and fuzzy logic are suitable for damage control problem, but they are very slow [7]. To some extent the speed of these approaches can be improved by using heuristics to reduce the search space. On the other hand expert system approaches are straight forward and fast [3]. But, its disadvantage is in difficulty to represent large system and designing an efficient inference engine for the large system [22].

### **2.3. Genetic Algorithm**

Genetic algorithm is a subset of evolutionary algorithms (EAs) that model biological processes to optimize highly complex cost functions [23]. Genetic algorithm is inspired from the mechanics of natural selection and natural genetics such as inheritance, mutation and recombination (also known as crossover). It is used in computing to find the optimal solutions to optimization and search problems.

Genetic algorithm was developed by John Holland in 1975 over the course of 1960s and 1970s [23]. Though the work of John Holland in development of genetic

algorithm is most significant, several other scientists were also involved in developing similar theories and algorithms. The ideas such as evolution strategy and evolutionary programming were also developed in 1960s by Ingo Rechenberg and Hans-Paul Schwefel in Germany and Lawrence Fogel and others in USA respectively. Both these methods incorporated the idea of mutation and selection from the neo-Darwinian theory of evolution. On the other hand only Bremerann and Fraser used the idea of recombination, the idea later placed at the heart of genetic algorithm by John Holland [19].

The solution space is encoded as strings of 0s and 1s for genetic algorithm implementation. Each string in the solution space is known as an individual or phenotype and a set of such individuals is called population. The genetic algorithm usually starts with a population of randomly generated individuals, which evolves generations based on genetic operations. In each generation, the fitness/objective function is evaluated for each individual present in the population. If the desired level of solution is not achieved, multiple individuals are stochastically selected (according to their fitness) from the current population and recombined to produce offspring. All offspring are mutated with a certain probability and then reinserted into the current population replacing the parents to produce a new generation of population. This process is repeated until the desired level of optimization is reached. This is known as single-population genetic algorithm. The structure of multi-population genetic algorithm is presented in Fig. 2.3.

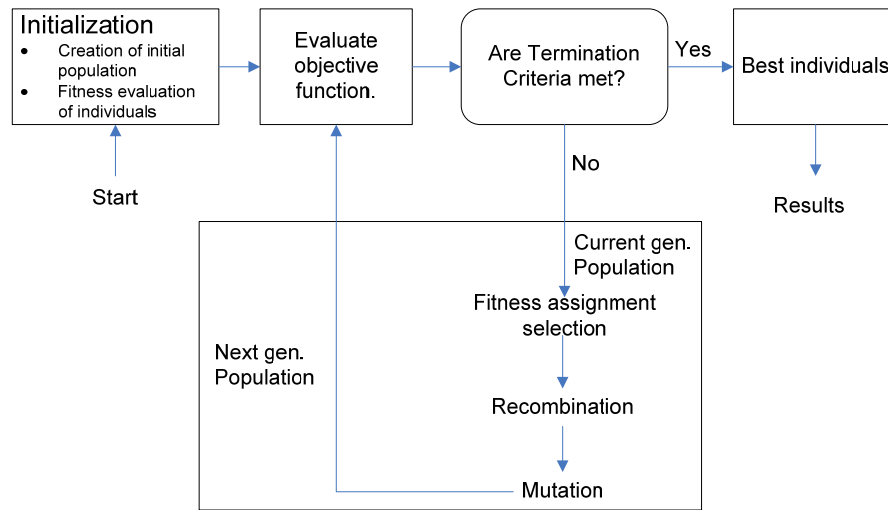


Fig.2.3. Structure of single-population genetic algorithm [24]

Single-population genetic algorithm performs well on a wide variety of problems. However, the use of multiple sub-populations improves the quality of solution obtained i.e. better fitness value and better solution speed. In multi-population genetic algorithm, every subpopulation initially evolves over a few generations isolated, before a few individuals are exchanged over the sub-populations. The structure of multi-population genetic algorithm is presented in Fig. 2.4.

The genetic algorithm differs substantially from the more traditional search and optimization methods. Some of the general observations about genetic algorithm are [25]:

- Genetic algorithm can rapidly find a good solution, even if the fitness function is multi-modal, discontinuous or does not have derivative over the solution space.

- Genetic algorithm A searches the solution space multiple points in parallel, instead of just a single point as done by traditional methods.
- Genetic algorithm as compared to traditional methods effectively solves the optimization problems with multiple objective functions.
- Genetic algorithm is based on probabilistic transition rules and not deterministic ones.

Genetic algorithms have a tendency to converge prematurely to a non-optimal point, rather than global optimal of the optimization problem. Therefore the diversity of the population is very important in genetic algorithms.

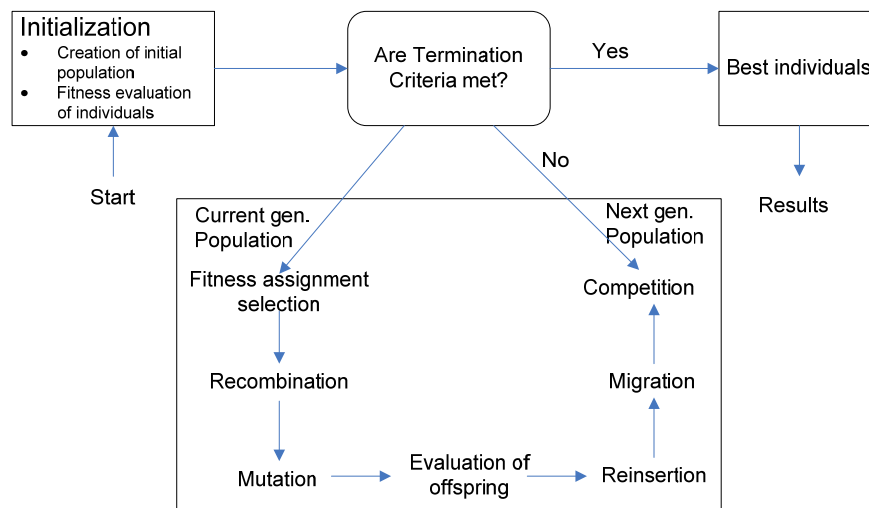


Fig.2.4. Structure of multi-population genetic algorithm [24]

### 3. PROBLEM FORMULATION

#### 3.1. Introduction

In the previous section, a notional NGIPS architecture was presented. The notional NGIPS consists of a HV/MV AC system and a DC zonal IFTP system, as shown in Fig. 2.2. In one possible solution, the dynamic damage control problem for NGIPS was formulated as constrained optimization problems for implementation at two different levels of the SPS: High/Medium Voltage (HV/MV) AC system and DC zonal Integrated Flight Through Power (IFTP) system. The optimal control problem was constrained by system operating conditions and system dynamics. Although, the dynamic damage control problem for NGIPS was formulated at two levels, the HV/MV AC system and the DC zonal IFTP system, this thesis discusses a genetic algorithm-based static implementation of the damage control method approach applied at the DC zonal IFTP system level for a notional NGIPS. The following sections present the mathematical problem formulation for the damage control method approach to a notional NGIPS DC zonal power system model.

#### 3.2. DC Zonal Power System Model

Fig. 3.1 shows a single zone of a DC zonal system of the notional NGIPS. The notional DC zonal system consists of  $N_z$  number of zones, each having two DC distribution buses, a starboard side bus and a port side bus. In Fig. 3.1, only the model of

one zone and the connections to other zones are shown. Each zone is served by a PCM-4, which supplies power to the DC distribution buses. A 4.16 kV AC, 60 Hz source, modeling the connection to the HV/MV AC system, is connected upstream of the PCM-4. Each distribution bus in a zone is connected to a PCM-1 module, shown with bold dotted line in Fig. 3.1, which supplies power to the loads in a zone through  $N_C^{Zn}$  number of power conversion functions (shown as DC-DC convertors  $Conv_{Si}^{Zn}$  and  $Conv_{Pj}^{Zn}$ ), where  $Zn$  is the zone number and  $C$  represents the conversion function. PCM-1s convert 1 kV DC distribution voltage to 375 V DC, 650 V DC, and 800 V DC levels. Each PCM-1 supplies power to various types of loads: non-vital DC loads, vital DC loads, non-vital AC loads, and vital AC loads. The starboard side bus  $i^{th}$  DC-DC power conversion function supplies power to  $N_{SiDC\_NVL}^{Zn}$  number of non-vital DC loads,  $N_{SiAC\_NVL}^{Zn}$  number of non-vital AC loads,  $N_{ijDC\_VL}^{Zn}$  number of vital DC loads, and  $N_{ijAC\_VL}^{Zn}$  number of vital AC loads, where  $j$  represents the corresponding power conversion function on the port side bus, such that  $i = j$ . Similarly, the port side bus  $j^{th}$  power conversion function supplies power to  $N_{PjDC\_NVL}^{Zn}$  number of non-vital DC loads,  $N_{PjAC\_NVL}^{Zn}$  number of non-vital AC loads,  $N_{ijDC\_VL}^{Zn}$  number of vital DC loads, and  $N_{ijAC\_VL}^{Zn}$  number of vital AC loads, where  $i$  represents the corresponding power conversion function on the starboard side bus, such that  $j = i$ . The PCM-1s are connected to the 450 V AC loads via PCM-2s, which convert the 800 V DC to 450 V AC.

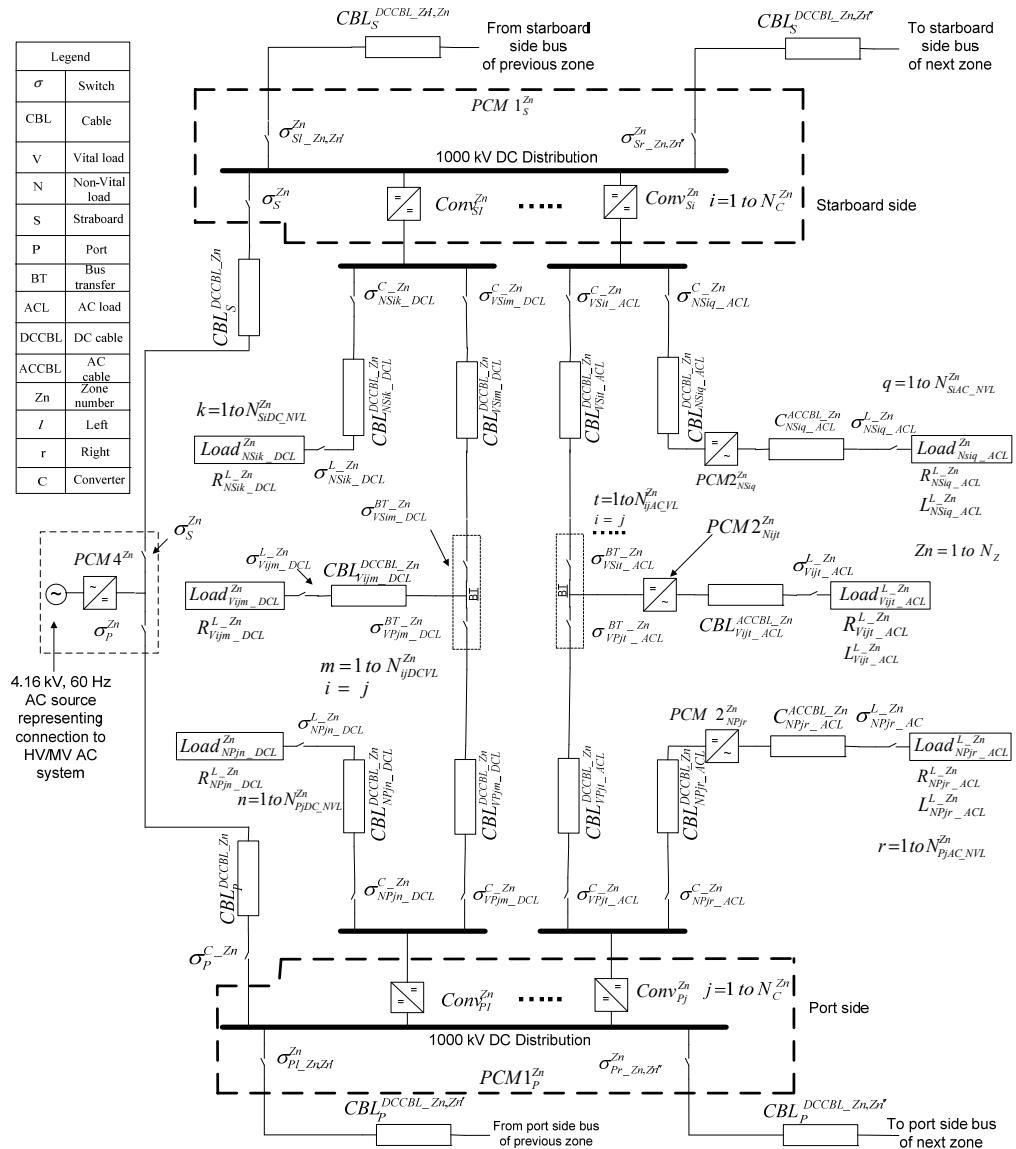


Fig. 3.1. Notional NGIPS DC zonal IFTP system

All AC/DC vital loads in the notional power system have two possible supply paths, which are connected by bus transfer switches. In case the normal supply path voltage dips below tolerance limits, the vital load supply path is switched by its associated bus transfer to its alternate supply path. The DC loads were modeled as

constant resistance and the AC loads were modeled as constant impedance loads. Both DC and AC cables were modeled using a lumped parameter model using resistance and self-inductance of the cables only.

### **3.3. Analytical Formulation of Dynamic Damage Control Method for DC Zonal System**

The damage control method is launched in response to system disturbances (representing a fault or battle damage) in the DC zonal power system. In response to the disturbance, the protective devices isolate the faulted sections. As a result, some of the vital and/or non-vital loads may be de-energized. The damage control method restores as many loads as possible without violating the system operating and dynamic constraints. In case of power capacity violations, the damage control algorithm sheds non-vital loads in order to restore vital loads in the DC zonal power system

The dynamic damage control problem for the DC zonal IFTP system was formulated by the PSAL research team as a constrained optimization problem. The system dynamics (DAEs) and system operating limits are the constraints in the mathematical problem formulation. The mathematical model for the dynamic damage control problem is shown in (3.1)-(3.10), with the objective function in (3.1), operating constraints in (3.2)-(3.8), and system dynamic constraints in (3.9)-(3.10). The objective of the damage control problem is to energize as many of the loads that were energized before the fault, considering the priority of the loads. This objective is accomplished mathematically by minimization of the weighted summation of absolute differences

between pre-fault load current values  $I_i^{nom}(\Delta t)$  and the optimal load current values  $I_i(\Delta t)$  as shown in (3.1). This mathematical model is applicable for the starboard-port side topology of the SPS. For other topologies, such as forward-aft, common bus, or split bus of SPS, the PCM-4 switch constraints and PCM-4 power capacity constraints will need to be modified.

$$Obj. func. \quad Min \quad f(\mathbf{I}(\Delta t), \boldsymbol{\sigma}) = \sum_{i=1}^{NL} W_i |I_i(\Delta t) - I_i^{nom}(\Delta t)| \quad (3.1)$$

$\mathbf{I}(\Delta t)$  represents the vector of average/RMS cable post-fault currents computed over time interval  $\Delta t$ , and  $\boldsymbol{\sigma}$  is the vector of switch status controlled by this method.  $W_i$  is the weight assigned to the  $i^{th}$  load.  $I_i(\Delta t)$  is the average/RMS current of the  $i^{th}$  DC/AC load over time  $\Delta t$ , for the candidate network configuration,  $I_i^{nom}(\Delta t)$  is the average/RMS pre-fault current for the  $i^{th}$  DC/AC load over time  $\Delta t$ , NL is the number of loads, and  $\Delta t$  is the time interval over which average and RMS values for variables are calculated.

B and N represent the set of all DC buses and set of all load nodes, respectively, in node voltage constraints (3.2)-(3.3), C represents the set of cables in cable ampacity constraints (3.4), T represents the set of bus transfer switches in switch constraints (3.7), and P represents the set of PCM-4 switches in PCM-4 power capacity constraints (3.5) and switch constraints (3.8). The objective function is subject to:

- a) *Node voltage constraints*: voltage at all DC buses including load node should be within tolerable limits:

$$V_k^{Bus\_min} \leq V_k^{Bus}(\Delta t) \leq V_k^{Bus\_max} \text{ for } k \in B \quad (3.2)$$

where  $V_k^{Bus}(\Delta t)$  is the  $k^{th}$  bus average/RMS voltage over time  $\Delta t$ , and  $V_k^{Bus\_min}$  and  $V_k^{Bus\_max}$  are the minimum and maximum average/RMS tolerable limits for the  $k^{th}$  bus voltage, respectively.

$$V_l^{load\_min} \leq V_l^{load}(\Delta t) \leq V_l^{load\_max} \text{ for } l \in N \quad (3.3)$$

where  $V_l^{load}(\Delta t)$  is the average/RMS voltage over time  $\Delta t$  at the  $l^{th}$  load node, and  $V_l^{load\_min}$  and  $V_l^{load\_max}$  are the minimum and maximum average/RMS tolerable limits for the  $l^{th}$  load node voltage, respectively.

- b) *Cable current ampacity constraints*: the current through cables should not exceed their ampacity ratings:

$$I_m^{Cable}(\Delta t) \leq I_m^{Cable\_max} \text{ for } m \in C \quad (3.4)$$

where  $I_m^{Cable}(\Delta t)$  is the average/RMS current for the  $m^{th}$  DC/AC cable over time  $\Delta t$ , and  $I_m^{Cable\_max}$  is the ampacity limit for the  $m^{th}$  DC/AC cable.

- c) *PCM-4 capacity constraints*: at any time, the power supplied by the PCM-4s should be within tolerable limits:

$$P_n^{PCM4}(\Delta t) \leq P_n^{PCM4_{max}} \text{ for } n \in P \quad (3.5)$$

where  $P_n^{PCM4}(\Delta t)$  is the average power supplied by the  $n^{th}$  PCM-4 over time  $\Delta t$ , and  $P_n^{PCM4_{max}}$  is the power rating for the  $n^{th}$  PCM-4.

The total demand and losses of the DC zonal system should not exceed the combined maximum capacity of all PCM-4s present in this system:

$$P_{loss}(\Delta t) + P_d(\Delta t) \leq \sum_{n=1}^{N_z} P_n^{PCM4_{max}} \quad (3.6)$$

where  $P_{loss}(\Delta t)$  and  $P_d(\Delta t)$  are, respectively, the average power loss and average power demand of the power system network computed over time  $\Delta t$ .

- d) *Switch constraints*: the BTs are modeled as a set of two switches, as shown in Fig. 3.2. It should be ensured that at any given time, both switches should not be closed.

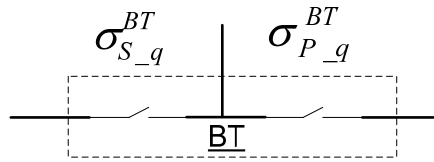


Fig. 3.2. Bus transfer switch

$$\sigma_{Sq}^{BT} \text{ AND } \sigma_{Pq}^{BT} \neq 1, \text{ for } q \in T \quad (3.7)$$

where  $\sigma_{Sq}^{BT}$  and  $\sigma_{Pq}^{BT}$  represent the starboard side and port side switches of a bus transfer switch, respectively.  $\sigma$  is a binary variable.

A similar condition applies to the PCM-4 switches for starboard/port configuration. The PCM-4 switches should remain in the starboard port topology in the post-fault configuration of the SPS. For other topologies, such as forward-aft, common bus, or split bus of SPS this constraint needs to be changed

$$\sigma_{Sn}^{PCM4} \text{ AND } \sigma_{Pn}^{PCM4} \neq 1, \text{ for } n \in P \quad (3.8)$$

where  $\sigma_{Sn}^{PCM4}$  and  $\sigma_{Pn}^{PCM4}$  represent the starboard side and port side switches of a PCM-4, respectively.  $\sigma$  is a binary variable.

- e) *System dynamics constraints (DAEs)*: the solution to the optimization problem should satisfy the system dynamic equations, which are represented by DAEs. Equations 3.9 and 3.10 represent the general structure for DAEs used.

$$\dot{\mathbf{x}}(t) = \mathbf{f}(\mathbf{x}(t), \mathbf{u}(t), \boldsymbol{\sigma}) \quad (3.9)$$

$$0 = \mathbf{g}(\mathbf{x}(t), \mathbf{u}(t), \boldsymbol{\sigma}) \quad (3.10)$$

where  $\mathbf{x}$  is the state vector of the system,  $\boldsymbol{\sigma}$  is the vector of switch status,  $\mathbf{u}$  is the vector of control input to the system, and  $t$  is the time.  $\mathbf{f}$  represents the vector of differential equations, and  $\mathbf{g}$  represents the vector of algebraic equations.

The solution to the mathematical problem formulation presented above will restore the power supply to as many loads as possible based on the weights assigned to the load. The feasible solution will also satisfy voltage, current, capacity, switch, and system dynamic constraints.

#### **3.4. Genetic Algorithm-Based Damage Control Method for DC Zonal System**

A genetic algorithm-based static damage control was implemented as a part of this research work, which is explained in the next section. The static damage control implementation is based on the other formulation except that the dynamic constraints were not included.

#### **3.5. Summary**

Section 3 provided an overall view of damage control problem formulation and presented the dynamic damage control problem formulation for the next generation SPS DC zonal IFTP system. The next section describes the static implementation based on the above described problem formulation.

## **4. IMPLEMENTATION DETAILS: GENETIC ALGORITHM-BASED DAMAGE CONTROL METHOD**

### **4.1. Introduction**

The notional next generation DC zonal power system model and mathematical problem formulation for a static damage control problem were presented in Section 3. The problem was formulated as an optimization problem with power system operating limits and dynamics as the constraints. Though the problem formulation presented in Section 3 is dynamic in nature, the damage control method implemented is static in nature. The genetic algorithm method solves the damage control problem as a combinatorial optimization problem. The power system operating constraints in the damage control problem are included in the objective function using penalty factors. The dynamic of system defined by DAEs are not used as constraints in the method. Instead the DAEs are used to find various power system variables, such as node voltages, cable currents to compute the objective function. The details of the genetic algorithm-based static implementation solution technique used for damage control in DC zonal IFTP system of NGIPS is presented in this section.

### **4.2. Damage Control Algorithm Module**

This section of the work discusses the details of the static implementation of the genetic algorithm-based damage control method. Fig. 4.1 presents a block diagram for

the damage control method. It takes the pre/post-fault system information as input and tries to find an optimal network configuration that restores the power system without violating the power system operating constraints. The optimal network configuration is the output of the damage control method. The damage control method module consists of two sub-modules: genetic algorithm sub-module and DAE solver and system operating constraints sub-module as shown in Fig. 4.1. The genetic algorithm sub-module generates various candidate solutions (network configurations), which are evaluated based on the objective function values as shown in Fig. 4.1. The variables in the objective function are computed by DAE solver and system operating constraints sub-module. Details of these modules are presented in Section 4.2.1 and 4.2.2.

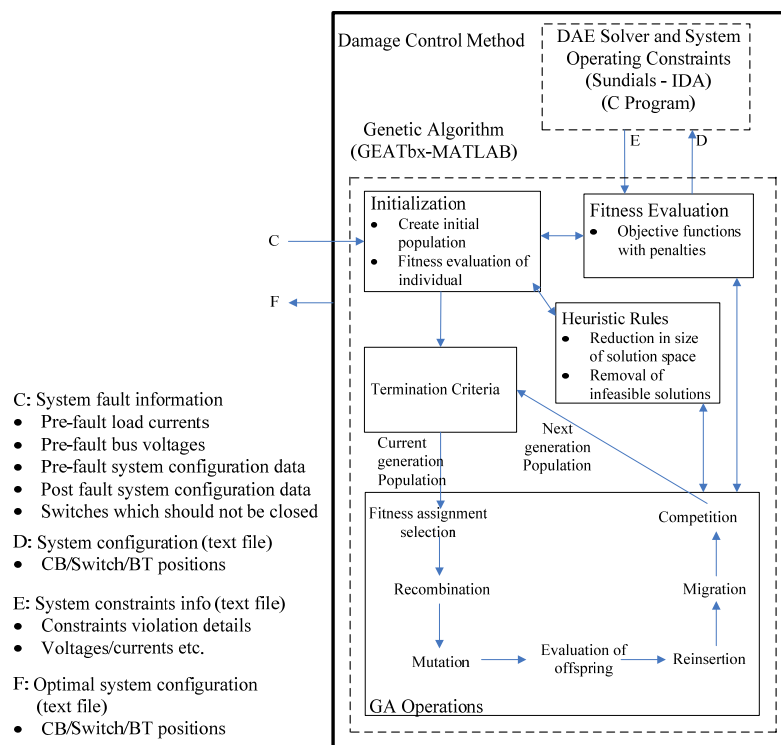


Fig. 4.1. Problem implementation: block diagram for damage control

#### 4.2.1. Genetic Algorithm Sub-Module

Genetic algorithm is a subset of evolutionary algorithms that model biological processes to optimize complex cost functions [23]. Genetic algorithm is inspired from the mechanics of natural selection and natural genetics, such as inheritance, mutation, and recombination. Genetic algorithm is used to find the optimal or sub-optimal solutions for optimization and search problems.

This sub-module implements the optimization problem stated in (3.1) using genetic algorithm. A constrained binary coded multi-population genetic algorithm with repair functions modeled as heuristic rules was used in this implementation. The genetic algorithm sub-module was implemented using GEATbx v.3.8 [26], MATLAB-based software.

The overall flow for the genetic algorithm sub-module is shown in Fig. 4.2. The genetic algorithm process starts with generation of an initial population of individuals which goes through a repair-and-replace process. Then the first generation of population is evaluated and termination conditions are checked. In case termination conditions are met, the best solution is stored in a text file and the method is terminated. Otherwise, the population goes through a selection process, in which few individuals are selected for the recombination process to generate new individuals. The population goes through a mutation process after recombination to increase the diversity in the population and avoid pre-mature convergence to a non-optimal solution. The objective function for these new individuals are evaluated and based on the objective function values these individuals are reinserted into the population. This is followed by the migration process,

where few individual from one sub-population migrate to another sub-population. These above mentioned set of processes leads to next generation of population for which the termination conditions are checked. If the termination conditions are not met, the population again goes through the series of processes, selection, recombination, mutation, function evaluation, reinsertion, and migration to generate a new population. Otherwise, the optimal network configuration is stored in a text file and the method is terminated. The optimal configuration stored in the text file is then applied to the power system model in PSCAD to check whether the results obtained by damage control method are correct or not.

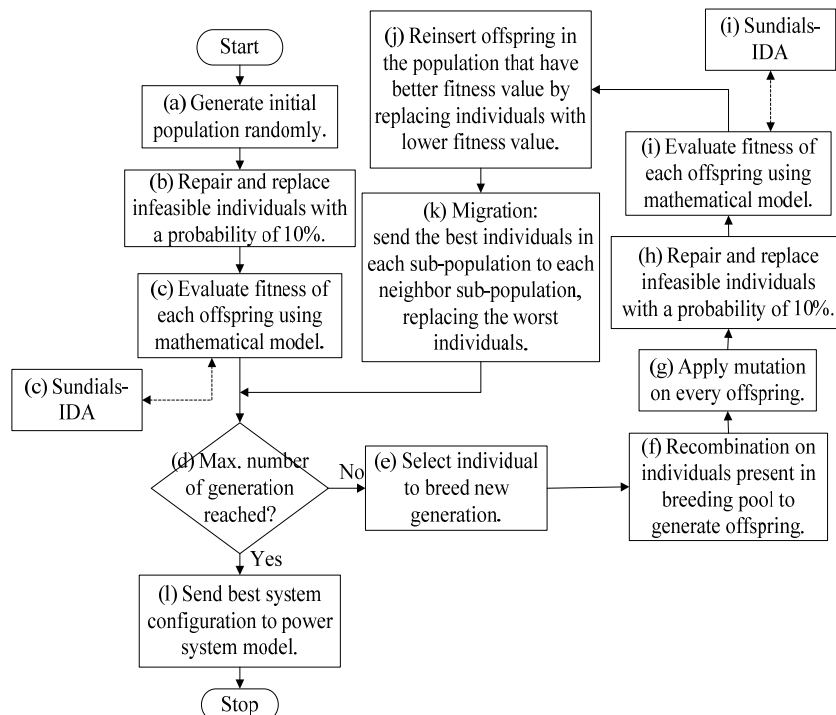


Fig. 4.2. Genetic algorithm sub-module flow chart

#### 4.2.1.1. Initialization

The first process in any genetic algorithm is initialization as shown in Fig. 4.2 as box (a). At the initialization step, the population, a set of randomly generated individuals also known as chromosomes, is constructed [24]. A binary string is used as an individual, which represents the status of all switches in the SPS that are controlled by the damage control method. Each binary number (gene) in the individual represents a switch position: “0” represents open and “1” represents closed. This chromosome forms the first generation of the population, which evolves over generations to reach an optimal solution, if possible. A multi-population model is used for this project. This means that the population consists of various small sub-populations. The number of sub-populations and number of individuals in per sub-population is calculated as:

$$\text{Number of sub - populations} = \text{floor}(\sqrt{\text{Number of variables}}), \quad (4.1)$$

$$\text{Number of individuals in eah sub - populations} = 20 + 5 * \text{floor}\left(\frac{\text{Number of variables}}{50}\right) \quad (4.2)$$

where, number of variables is equal to the number of switches present in the power system.

A general structure for a chromosome for the notional DDIPS DC zonal system developed is shown in Fig. 4.3. Fig. 4.4, Fig. 4.5, Fig. 4.6, Fig. 4.7, Fig. 4.8, and Fig. 4.9 presents the details of the structure of the chromosome for one zone.

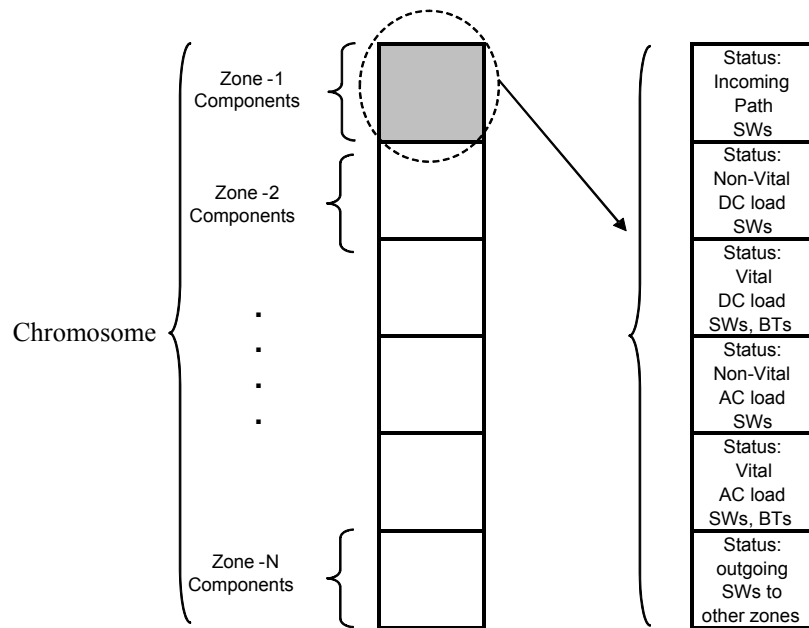


Fig. 4.3. Overall chromosome structure for notional DC zonal system

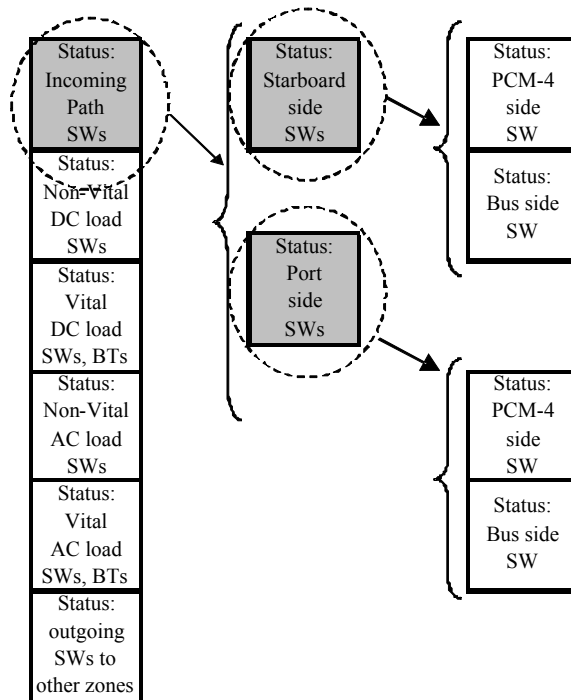


Fig. 4.4. Chromosome structure for one zone: incoming switches

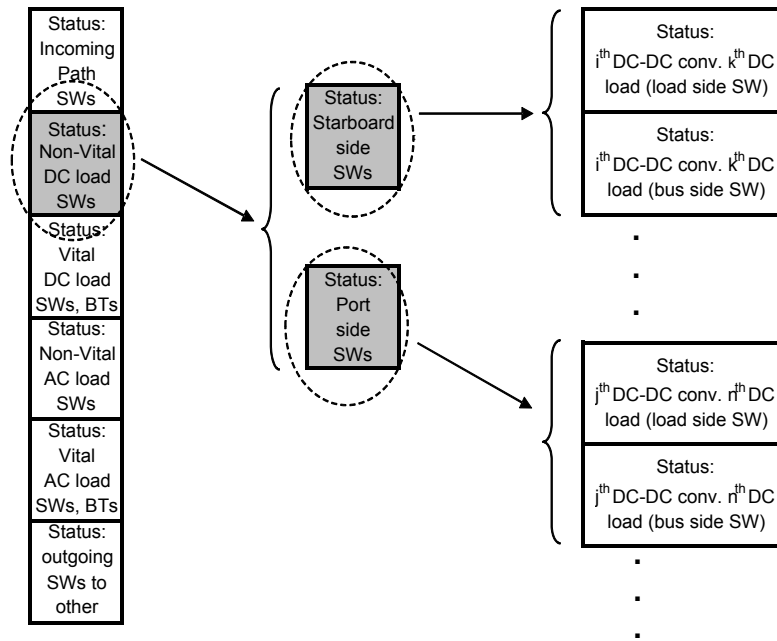


Fig. 4.5. Chromosome structure for one zone: non-vital DC load switches

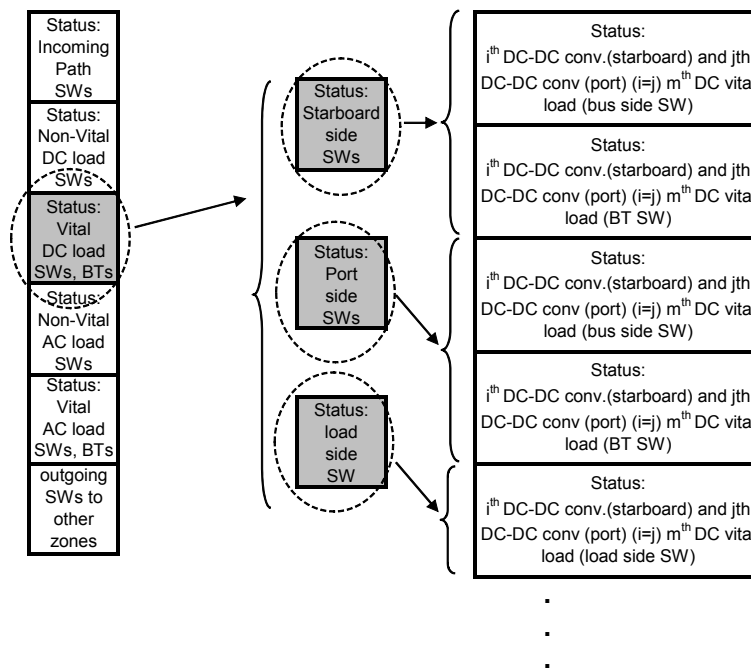


Fig. 4.6. Chromosome structure for one zone: vital DC load switches

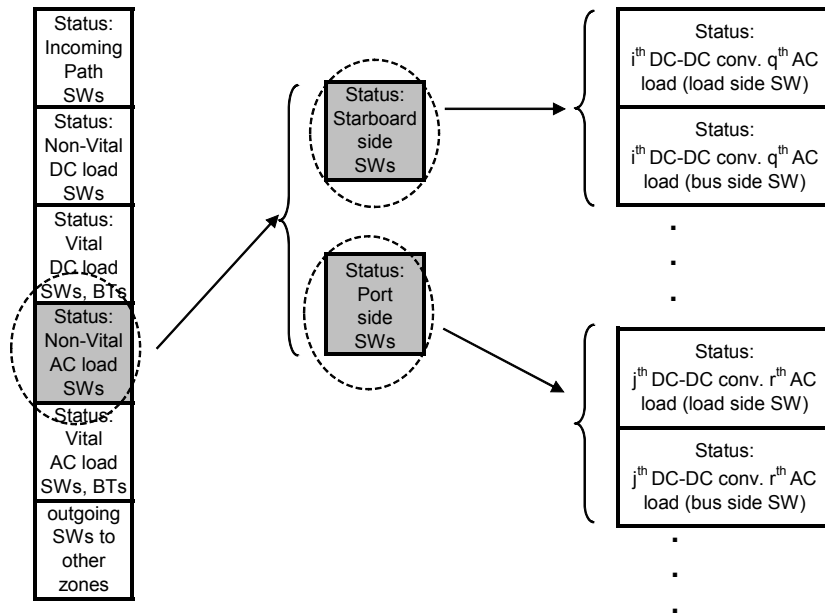


Fig. 4.7. Chromosome structure for one zone: non-vital AC load switches

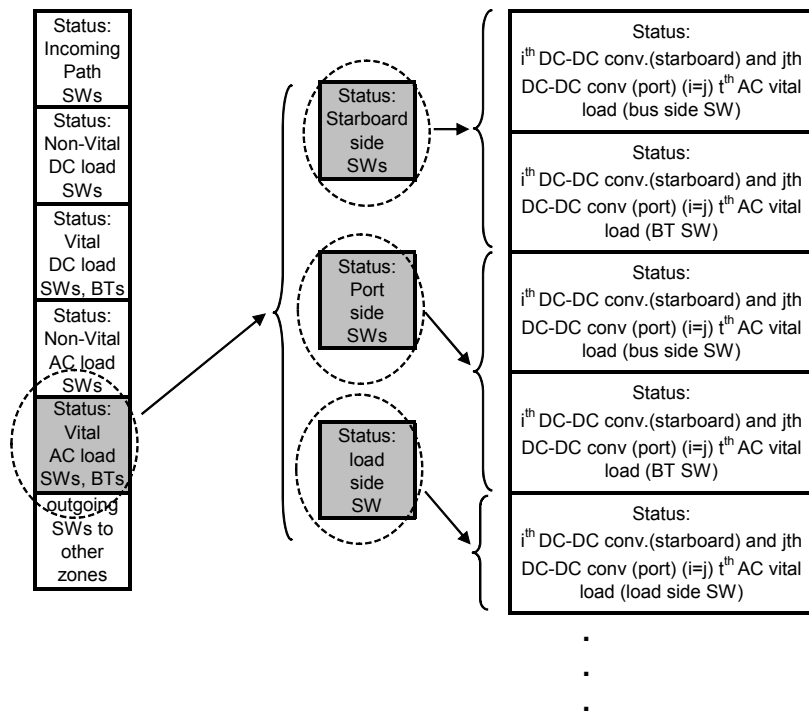


Fig. 4.8. Chromosome structure for one zone: vital AC load switches

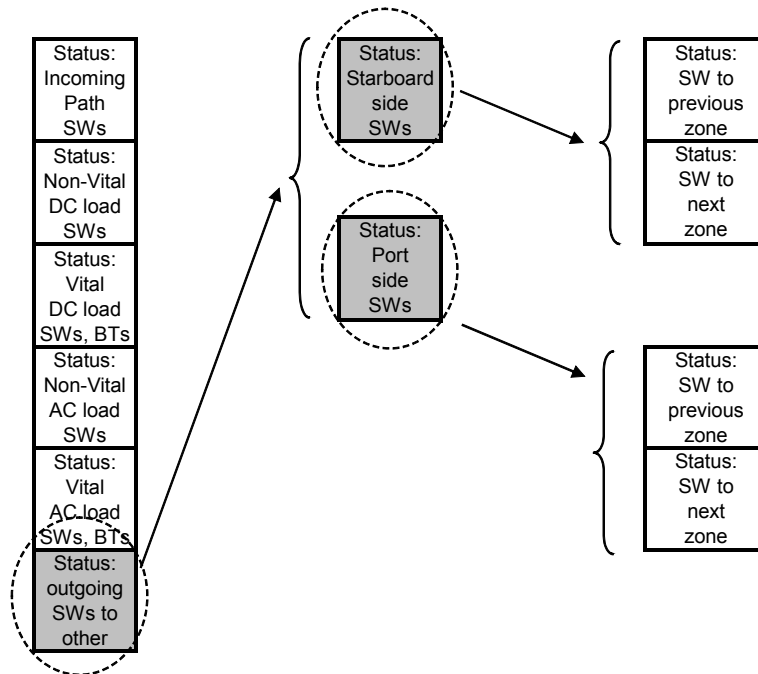


Fig. 4.9. Chromosome structure for one zone: outgoing switches

#### 4.2.1.2. Repair-and-Replace Process

Boxes (b) and (h) represent the repair and repair process in Fig. 4.2. After a population is created, the population is passed through a repair-and-replace process. The repair process picks out the infeasible individuals, individuals with switch constraint violations, and converts them into feasible ones by removing the switch constraint violation [27]. 10% of the individuals are randomly selected from the set of repaired individuals and are returned to the population replacing their infeasible counterpart. Use of the repair-and-replace strategy improves the convergence rate and solution quality [27]. The repair operators used for this problem formulation consisted of the switch constraints, described in Section 2, and the constraint on switches that should not be

closed in order to keep the faulted section isolated from the rest of the system. If any of the above mentioned switch constraints are violated, the individual is considered infeasible and needs to go through the repair process. The repair process is applied to the population after the initialization and mutation stages.

If any of the switch constraints are violated, the individual is considered as infeasible and needs to go through the repair process. The repair process is applied to the population after the initialization and mutation. In case an individual does not satisfy any of the switch constraints, it is repaired and replaced in the population with a probability of 10%.

Any switch, which when closed, connects the faulted section back to the rest of the power system, and makes the system unstable, should not be closed. The list of switches which should be closed by the damage control algorithm is provided by pre/post-fault info extractor based on the list of faulted components. The switches which should not be closed are assigned a value equal to '1'. This is compared with the network configuration provided by the genetic algorithm. In case, any of the above mentioned switches in the individual are closed, the network configuration is considered infeasible. These individuals can be repaired by changing the status of the switches to '0'. Fig. 4.10 shows an example of an infeasible individual.

|                           |   |   |   |   |   |   |   |     |
|---------------------------|---|---|---|---|---|---|---|-----|
| Individual                | 1 | 0 | 0 | 1 | 0 | 1 | 1 | ... |
| Switches not<br>be closed | 0 | 0 | 1 | 1 | 0 | 0 | 0 | ... |

Fig. 4.10. Switches not to be closed

At any moment of time PCM-4 should be connected to one and only one bus i.e. starboard side or port side bus in a zone for the starboard/port bus topology of the ship. An example of this constraint for PCM-4 for zone  $Z_n$  is shown in (4.3). Fig. 4.11 shows the PCM-4 switches.

$$\sigma_S^{Sr-Zn} \text{ AND } \sigma_P^{Sr-Zn} \neq 1, \text{ where } Zn = 1 \text{ to } N_z \quad (4.3)$$

where,  $\sigma_S^{Sr-Zn}$  and  $\sigma_P^{Sr-Zn}$  represents the PCM-4 switches for zone  $Z_n$ .

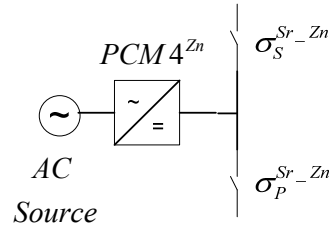


Fig. 4.11. PCM-4 switches

DC vital load bus transfers are modeled as set of two switches similar to PCM-4 switches. Therefore, any individual which have DC load bus transfer switch status as (1, 1) is considered infeasible. An example of this constraint for DC load bus transfer switches for zone  $Z_n$  is shown in (4.4).

$$\sigma_{VSim\_DCL}^{BT-Zn} \text{ AND } \sigma_{VPjm\_DCL}^{BT-Zn} \neq 1, \text{ where } Zn = 1 \text{ to } N_z, i = j = 1 \text{ to } N_C^{Zn}, m = 1 \text{ to } N_{ijDC\_VL}^{Zn} \quad (4.4)$$

where,  $\sigma_{VSim\_DCL}^{BT\_Zn}$  and  $\sigma_{VPjm\_DCL}^{BT\_Zn}$  represents the  $m^{th}$  DC vital load bus transfer starboard side and port side switches in zone  $Z_n$ .

AC vital load bus transfers are modeled as set of two switches similar to PCM-4 switches. Therefore, any individual which have AC load bus transfer switch status as (1, 1) is considered infeasible. An example of this constraint for AC load bus transfer switches for zone  $Z_n$  is shown in (4.5).

$$\sigma_{VSt\_ACL}^{BT\_Zn} \text{ AND } \sigma_{VPjt\_ACL}^{BT\_Zn} \neq 1, \text{ where } Zn = 1 \text{ to } N_z, i = j = 1 \text{ to } N_C^{Zn}, t = 1 \text{ to } N_{ijAC\_VL}^{Zn} \quad (4.5)$$

where,  $\sigma_{VSt\_DCL}^{BT\_Zn}$  and  $\sigma_{VPjm\_DCL}^{BT\_Zn}$  represents the  $t^{th}$  AC vital load bus transfer starboard side and port side switches in zone  $Z_n$ .

#### 4.2.1.3. Objective Function Evaluation

Boxes (c) and (i) represent the objective function evaluation process in Fig. 4.2. This process is divided into two sub-processes, solving DAEs to find out system variables and power system operating constraint violations in Sundial-IDA, general-purpose solver for the initial value problem for systems of DAEs, and computing the objective function value in GEATbx. Equations (4.6)-(4.13) show the objective function with penalty factors in the implementation. The purpose of penalty factors in the objective function is to eliminate the non-optimal solutions. The objective function is divided into two parts based on the switch constraint violations. When the switch

constraints are not violated, the static penalty factor  $PF_1$  as shown in (4.7) is summed with the function  $f$  to compute the objective function value as shown in (4.6). Otherwise, the objective function equals  $PF_2$  as shown in (4.9), which is a combination of static and dynamic penalty factors [28]. Therefore, the objective of this problem with penalty factors is to minimize the weighted summation of absolute differences between pre-fault load current values  $I^{nom}(\Delta t)$  and the load current values  $I(\Delta t)$  for the candidate network configuration along with the penalty factors  $PF_1$  and  $PF_2$ . The term  $PF_1$  consist of two terms, one related to the power system operating limit violation and second related to the number of switching actions required to reach the configuration proposed by genetic algorithm from the post-fault configuration of the power system. The term  $PF_2$  is made up of four terms, all related to switch constraint violations such as; PCM-4 switch status change (topology change), faulted section re-energization, PCM-4 switch constraint violation, and BT switch constraint violation etc., which make the individual infeasible

$$Obj.Func. \quad Min. \begin{cases} f(W, I(\Delta t), I^{nom}(\Delta t)) + PF_1, & \text{if } SW \\ & \text{constraints not violated} \\ PF_2, & \text{otherwise} \end{cases} \quad (4.6)$$

$$PF_1 = 2000 * A + 20 * N_{sw\_action} \quad (4.7)$$

$$A = \begin{cases} 0, & \text{if } \left\{ \begin{array}{l} V_{Bus\_min} < V_{Bus}(\Delta t) < V_{Bus\_max} \\ OR \\ I_{Cable}(\Delta t) < I_{Cable\_max} \\ OR \\ P_{PCM4\_min} < P_{PCM4}(\Delta t) < P_{PCM4\_max} \end{array} \right\} \\ 1, & \text{otherwise} \end{cases} \quad (4.8)$$

In (4.8),  $A$  represents any of the operating limit violations, and  $N_{sw\_action}$  is the number of switching actions required to reach the current switch configuration from post-fault configuration.  $I_{cable}(\Delta t)$  represents the vector of average/RMS cable currents computed over time interval  $\Delta t$ , and  $P_{PCM4}(\Delta t)$  represents the vector of average power for PCM-4s over time interval  $\Delta t$ .  $V_{Bus\_min}$  and  $V_{Bus\_max}$  represent the vectors of minimum and maximum average/RMS tolerance limits for voltages at buses and load nodes,  $I_{cable\_max}$  represents the vector of cable ampacity for all cables, and  $P_{PCM4\_max}$  represents the vector of power rating for PCM-4s. The penalty factor for  $A$  in function  $PF_1$  in (4.7) was selected in such a way that for any scenario, the term  $2000 * A$  is bigger than the term  $W|I(\Delta t) - I^{nom}(\Delta t)|$  for any load in the DC zonal power system. A small penalty factor was selected for the number of switching actions to avoid unnecessary load shedding.

$$PF_2 = (C + D + E)(10^4 + gen * 100) \quad (4.9)$$

$$B = \begin{cases} 0, & \{PCM - 4 \text{ switch status change} \\ 1, & \text{otherwise} \end{cases} \quad (4.10)$$

$$C = \begin{cases} 0, & \{faulted \text{ section re - energized} \\ 1, & \text{otherwise} \end{cases} \quad (4.11)$$

$$D = \begin{cases} 0, & \text{if PCM4 Switch constraint violated} \\ 1, & \text{otherwise} \end{cases} \quad (4.12)$$

$$E = \begin{cases} 0, & \text{if BT Switch constraint violated} \\ 1, & \text{otherwise} \end{cases} \quad (4.13)$$

In (4.9), represents PCM-4 switch status change, C represents a restoration action of a faulted section, D and E represent the PCM-4 switch and BT switch constraint violations, respectively, and gen is the current genetic algorithm generation. The penalty factors in function  $PF_2$  as shown in (4.9) were selected such that the objective function value achieved for an infeasible individual should always be higher than that for the feasible individual. Also, a dynamic term  $100 \cdot \text{gen}$  is added to the static penalty factor to force the genetic algorithm to search away from infeasible region as the genetic algorithm progresses through generations.

The vector of post-fault average/RMS cable current  $I(\Delta t)$  in the objective functions is computed using a set of DAE's, modeled in Sundials-IDA program, for the DC zonal system over time  $\Delta t$ . The computed post-fault average/RMS voltage and cable current vectors,  $V(\Delta t)$  and  $I(\Delta t)$ , respectively are compared against the operating limits in the Sundials-IDA, to determine the penalty factors to be used

#### 4.2.1.4. Selection

Box (e) represents the selection process in Fig. 4.2. In case the termination criterion is not met, 90% of the individuals in the population are selected for breeding offspring. Selection is the process of choosing the individuals for the recombination process and finding out how many offspring each selected individual will produce [24]. The selection process is based on the fitness of the individual. The first step in the selection process is the fitness assignment, which can be performed by one of

proportional fitness assignment method: rank-based fitness assignment, or multi-objective ranking method.

In this study, fitness values were computed by the linear rank based fitness assignment method. In rank based fitness assignment, the population is sorted according to the objective values and a fitness value is assigned to each individual based on the position of the individual in the list [24]. The rank-based method overcomes the scalability problem of the proportional fitness assignment method. Rank based fitness assignment method provides a uniform scaling across the population [24]. Selection pressure of 1.7 was used for the proposed damage control method implementation.

The second step in the selection process is the selection of parents, individuals selected for recombination process. This can be achieved by means of one of the algorithms: roulette-wheel selection, stochastic universal sampling, local selection, truncation selection, or tournament selection.

Tournament-based selection method is used in this implementation. In tournament selection a number *Tour* of individuals is chosen randomly from the population and the best individual from this group is selected as parent. This process is repeated as often as individuals must be chosen. These selected parents produce uniform at random offspring. The parameter for tournament selection is the tournament size *Tour*. *Tour* takes values ranging from 2 to *Nind* (number of individuals in population) [24]. *Tour* size of 5 is used in this project, which means about 50% of the population are lost. The loss of diversity is computed as:

$$LossDiv_{Turnier}(Tour) = Tour^{\frac{-1}{Tour-1}} - Tour^{\frac{-Tour}{Tour-1}} \quad (4.14)$$

#### 4.2.1.5. Recombination

Box (f) represents the recombination process in Fig. 4.2. Recombination, or crossover, is the process of producing new individuals by combining the information present in two or more parents [23]. As binary representation for the individual is used, the binary valued recombination is used for this project. This recombination can be performed by one of the methods: single/double/multi-point crossover, uniform crossover, shuffle crossover, or crossover with reduce surrogate method.

The double-point reduced surrogate crossover, a binary valued recombination, used for this research encourages the exploration of the search space, rather than favoring the pre-mature convergence, thus making the search more robust [24]. In double-point crossover the two point at which crossover happens are selected uniform at random and the information between the two individuals are exchanged to produce two offspring. The reduce surrogate method constrains the crossover to produce new offspring wherever possible. The recombination rate value is set as 0.7 for this project. In case very high value of recombination rate is used, the algorithm may converge prematurely to a non-optimal solution. Fig. 4.12 shows an example for multi-point crossover, where the vertical line represents the points at which crossover happens. This sub-module gets the chromosome from the main genetic algorithm program as an input, and gives back the updated chromosome.

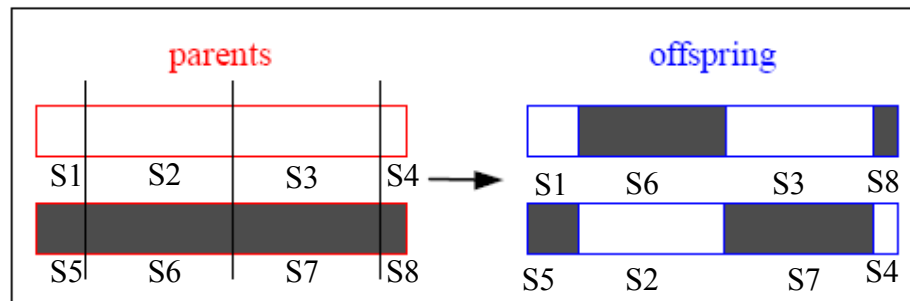


Fig. 4.12. Multi-point crossover

#### 4.2.1.6. Mutation

Box (g) represents the mutation process in Fig. 4.2. Mutation is the next process after recombination. Mutation is the process of altering the individuals randomly [23]. Normally, mutation is applied on the offspring generated by the recombination process. Binary valued mutation option is used for this project as the genes are represented in binary form. The mutation is defined with two parameters i.e. mutation step and mutation rate. For the binary valued mutation, mutation step is always 1 as each gene can have only two possible states i.e. 0 and 1. Mutation rate of 1 is selected, which means average 1 variable per individual is mutated. An example of binary mutation is given in Fig. 4.13, in which one of the binary number is gets changed from '1' to '0'.

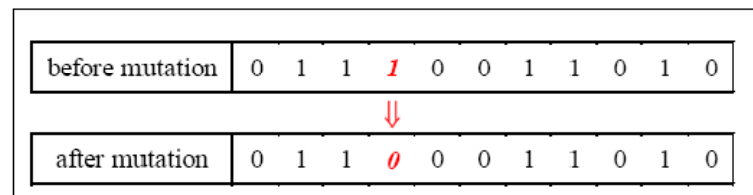


Fig. 4.13. Binary valued mutation

#### 4.2.1.7. Reinsertion

Box (j) represents the reinsertion process in Fig. 4.2. After the population has gone through selection, recombination, and mutation, the offspring need to be reinserted into the existing population, resulting in new generation of the population [24]. If the number of offspring is less than the number of individuals in the original population, then the size of the population is maintained. On the other hand, if more offspring are generated, the reinsertion scheme is used to replace individuals in the original population. GEATbx software provides two types of reinsertion method, global reinsertion and local reinsertion method.

For this project global reinsertion scheme is used. For this global reinsertion scheme only offspring fitter than weakest neighbor are reinserted, weakest neighbors are replaced. For this project elitist global reinsertion method was used, as shown in Fig. 4.14, where less number of offspring were produced than the parent individuals and the worst parent individuals were replaced [24]. The elitist combined with the fitness-based reinsertion prevents the loss of information [24].

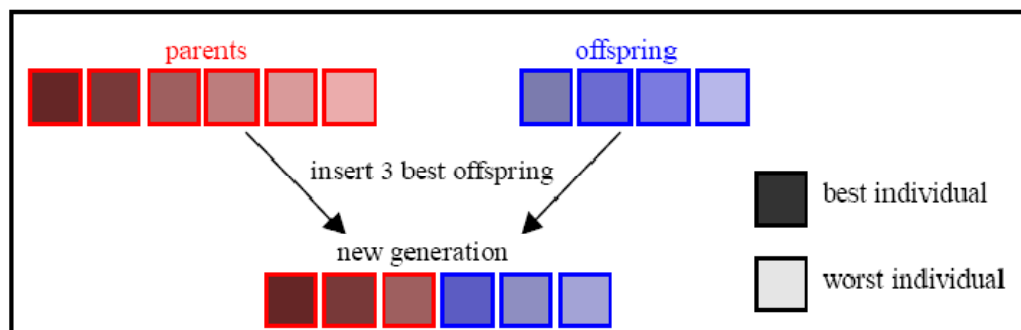


Fig. 4.14. Elitist reinsertion scheme

#### 4.2.1.8. Migration

Box (k) represents the migration process in Fig. 4.2. After the specified number of generations is completed, migration routine is called [24]. Migration is used in multi-population genetic algorithm. It divides the population into mutable sub-populations, which evolves independently over specified number of generations (isolation time). After the specified number of generations few individuals are exchanged between these sub-population based on the migration topology and migration rate used. There are three migration topologies present in GEATbx software. GEATbx software provides three migration topologies, unrestricted migration topology, ring topology, and neighborhood topology, to be used in genetic algorithm.

For this project an unrestricted migration topology is used, in which individuals migrates from any sub-population to another. A pool of best individuals from each sub-population is created from which individuals are selected based on the fitness value to replace the worst individuals in the other sub-populations. The migration improves the diversity of the population and helps in converging to a better solution. Migration interval was set to 20, which is the default value in the software. In case small value is used, it decreases the isolation of the individuals. Also, it is ensured that individuals are not imported back to the same sub-population. An illustration of the unrestricted migration topology with six sub-populations is shown in Fig. 4.15. The individuals can get exchanged between any two sub-populations.

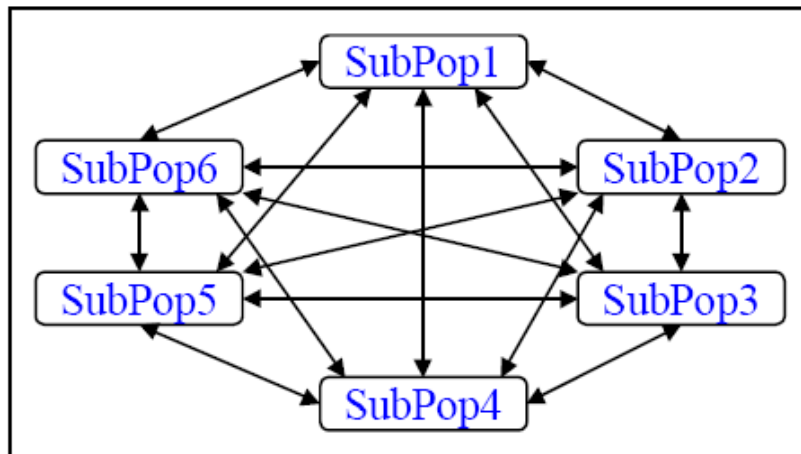


Fig. 4.15. Unrestricted migration topology

#### 4.2.2. DAE Solver and System Operating Constraints Sub-Module

The DAE solver and system operating constraints sub-module as shown in Fig. 4.1 computes the values of the node voltages, cable current and power flow for the candidate network configuration generated by genetic algorithm to determine if the soft constraints (3.2)-(3.8), switch constraints, bus/node voltage constraints, cable ampacity constraints, switch constraints, and PCM-4 capacity constraints are satisfied. The genetic algorithm sub-module calls the system constraints sub-module whenever the objective function needs to be evaluated for a feasible individual. The feasible individual representing a network configuration is applied to the DAE solver, which computes the various system variables, voltages, and currents over a time interval  $\Delta t$ . The system variables are then checked against soft constraints to check the feasibility of the solution obtained. The system variable values and the constraint violation details are sent back to the genetic algorithm sub-module, where the objective function value is evaluated.

The DAE solver and system operating constraints sub-module was modeled in Sundials-IDA v.2.5.0 [29], a general-purpose solver for the initial value problem for systems of DAEs. A DAE model of the power system in the general form used by IDA, shown in (4.13), was modeled. IDA uses the Newton/direct or Newton/Krylov methods to solve the DAEs. For this implementation the choice of Newton/direct method was made. For larger DAE systems the choice of Newton/Krylov method is better, but it requires a pre-conditioning matrix.

$$F(t, \mathbf{y}, \dot{\mathbf{y}}) = 0, \quad \mathbf{y}(t_0) = \mathbf{y}_0, \quad \dot{\mathbf{y}}(t_0) = \dot{\mathbf{y}}_0 \quad (4.15)$$

where  $\mathbf{y}$ ,  $\dot{\mathbf{y}}$ , and  $F$  are vectors of variables, their derivatives and system equations in  $\mathbf{R}^N$ ,  $t$  is the independent time variable, and  $\mathbf{y}_0$ , and  $\dot{\mathbf{y}}_0$  are the initial values of the variables and their derivative [29].

### 4.3. Summary

This section of the thesis presented a new genetic algorithm static implementation of damage control method. The details of various case studies conducted to test the proposed method is presented in next section.

## 5. CASE STUDIES AND SIMULATIONS

### 5.1. Introduction

This section of the work presents the off-line process used to test the genetic algorithm damage control method implementation discussed in the previous section. An overall block diagram for testing of the effectiveness of this damage control approach is shown in Fig. 5.1, which consists of four modules: power system simulation model, failure assessment module, pre/post-fault information extractor module, and damage control method module. In general, a fault scenario was simulated on the power system, and various system variables, such as node voltages, branch currents, and switch status, are recorded in a text file. The failure assessment module, implemented as a stub, provides the list of the faulted components in the power system network. This information along with the pre/post-fault system information is passed on to the damage control method module. The damage control method tries to find an optimal network configuration that restores the power system without violation of the power system operating constraints. The optimal network configuration is sent to the power system model.

### 5.2. Power System Simulation Model

A power system example based on the DC zonal system, presented in Section 3, was modeled in PSCAD software. Fig. 5.2 shows a figure of the power system example.

The power system example consists of two zones, each having one DC-DC converter connected to starboard and port buses. For simplicity, the AC source and the PCM-4 are modeled as a DC source. Zone-1 consists of one DC non-vital load and three vital loads. Zone-2 consists of two DC non-vital loads and two DC vital loads. AC loads and PCM-2s are not included in the model. Table 5.1 and Table 5.2 present the details for the loads and cables used for the power system example, respectively. The system measurements for a scenario, such as node voltages, branch currents, and switch status, are stored in a text file, which is passed on to the failure assessment module and pre/post-fault information extractor module.

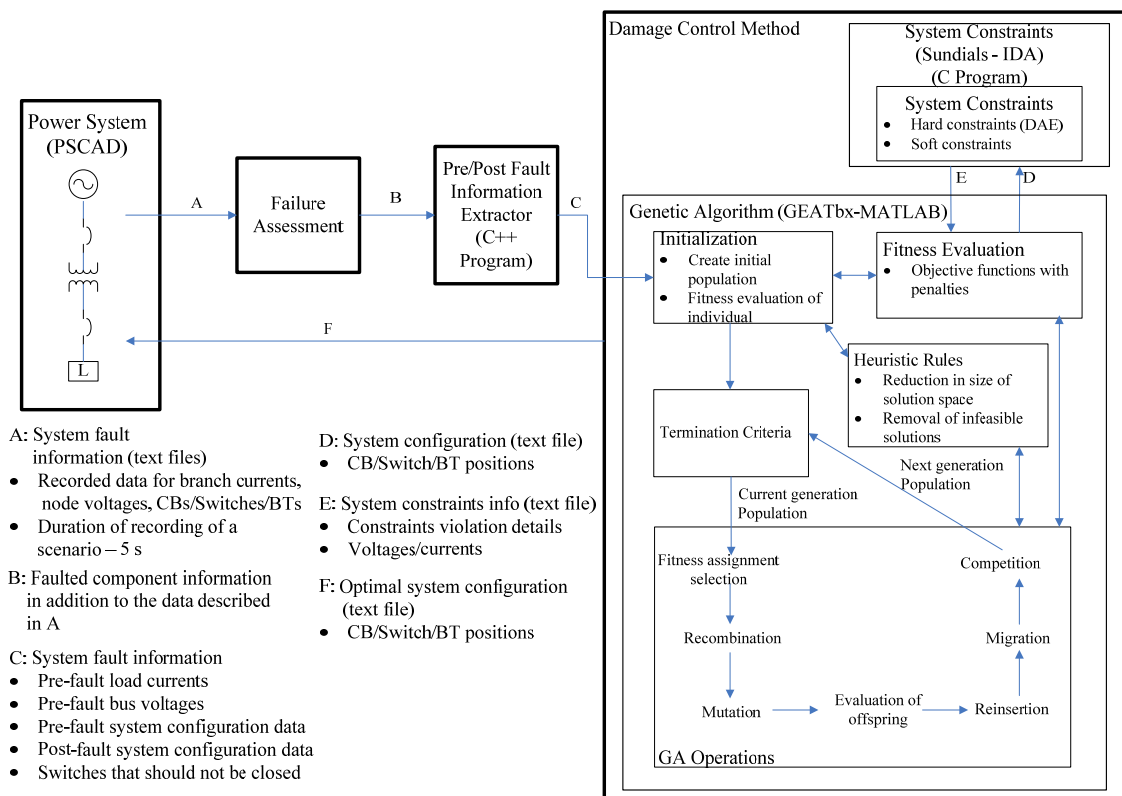


Fig. 5.1. Problem implementation: off-line process to test the damage control method

Table 5.1. Power system example: load details

| Load Name       | Load Type | weight factor | Rated power (kW) | Rated Voltage (V) | R ( $\Omega$ ) |
|-----------------|-----------|---------------|------------------|-------------------|----------------|
| Load 1 NP11 DCL | NV        | 2.00          | 175              | 650               | 2.41           |
| Load 1 V111 DCL | V         | 2.58          | 300              | 650               | 1.41           |
| Load 1 V112 DCL | V         | 2.58          | 300              | 650               | 1.41           |
| Load 1 V113 DCL | V         | 3.00          | 175              | 650               | 2.41           |
| Load 2 NS11 DCL | NV        | 2.00          | 175              | 650               | 2.41           |
| Load 2 NP11 DCL | NV        | 2.00          | 175              | 650               | 2.41           |
| Load 2 V111 DCL | V         | 2.58          | 300              | 650               | 1.41           |
| Load 2 V112 DCL | V         | 2.58          | 300              | 650               | 1.41           |

Table 5.2. Power system example: cable details

| Sr. No. | Cable Name       | Cable Description      | Length (m) | Cable resistance (ohm) | Cable Inductance (H) | Cable Ampacity (A) |
|---------|------------------|------------------------|------------|------------------------|----------------------|--------------------|
| 1       | DCCBL_1_SRBT     | 2 runs, 350 kemil, 1kV | 20         | 1.35E-04               | 1.68E-05             | 1140               |
| 2       | DCCBL_1_PRBT     | 2 runs, 350 kemil, 1kV | 20         | 1.35E-04               | 1.68E-05             | 1140               |
| 3       | DCCBL_1_NP11_DCL | 1 run, 4/0, 1kV        | 15         | 4.35E-04               | 2.57E-05             | 405                |
| 4       | DCCBL_1_VS11_DCL | 1 run, 350 kemil, 1kV  | 15         | 1.46E-03               | 5.22E-05             | 570                |
| 5       | DCCBL_1_VP11_DCL | 1 run, 350 kemil, 1kV  | 15         | 1.46E-03               | 5.22E-05             | 570                |
| 6       | DCCBL_1_V111_DCL | 1 run, 350 kemil, 1kV  | 15         | 1.46E-03               | 5.22E-05             | 570                |
| 7       | DCCBL_1_VS12_DCL | 1 run, 350 kemil, 1kV  | 15         | 1.46E-03               | 5.22E-05             | 570                |
| 8       | DCCBL_1_VP12_DCL | 1 run, 350 kemil, 1kV  | 15         | 1.46E-03               | 5.22E-05             | 570                |
| 9       | DCCBL_1_V112_DCL | 1 run, 350 kemil, 1kV  | 15         | 1.46E-03               | 5.22E-05             | 570                |
| 10      | DCCBL_1_VS13_DCL | 1 run, 4/0, 1kV        | 15         | 4.35E-04               | 2.57E-05             | 405                |
| 11      | DCCBL_1_VP13_DCL | 1 run, 4/0, 1kV        | 15         | 4.35E-04               | 2.57E-05             | 405                |
| 12      | DCCBL_1_V113_DCL | 1 run, 4/0, 1kV        | 15         | 4.35E-04               | 2.57E-05             | 405                |
| 13      | DCCBL_12_S       | 2 runs, 350 kemil, 1kV | 20         | 1.35E-04               | 1.68E-05             | 1140               |
| 14      | DCCBL_12_P       | 2 runs, 350 kemil, 1kV | 20         | 1.35E-04               | 1.68E-05             | 1140               |
| 15      | DCCBL_2_SRBT     | 2 runs, 350 kemil, 1kV | 20         | 1.35E-04               | 1.68E-05             | 1140               |
| 16      | DCCBL_2_PRBT     | 2 runs, 350 kemil, 1kV | 20         | 1.35E-04               | 1.68E-05             | 1140               |
| 17      | DCCBL_2_NS11_DCL | 1 run, 4/0, 1kV        | 15         | 4.35E-04               | 2.57E-05             | 405                |
| 18      | DCCBL_2_NP11_DCL | 1 run, 4/0, 1kV        | 15         | 4.35E-04               | 2.57E-05             | 405                |
| 19      | DCCBL_2_VS11_DCL | 1 run, 350 kemil, 1kV  | 15         | 1.46E-03               | 5.22E-05             | 570                |
| 20      | DCCBL_2_VP11_DCL | 1 run, 350 kemil, 1kV  | 15         | 1.46E-03               | 5.22E-05             | 570                |
| 21      | DCCBL_2_V111_DCL | 1 run, 350 kemil, 1kV  | 15         | 1.46E-03               | 5.22E-05             | 570                |
| 22      | DCCBL_2_VS12_DCL | 1 run, 350 kemil, 1kV  | 15         | 1.46E-03               | 5.22E-05             | 570                |
| 23      | DCCBL_2_VP12_DCL | 1 run, 350 kemil, 1kV  | 15         | 1.46E-03               | 5.22E-05             | 570                |
| 24      | DCCBL_2_V112_DCL | 1 run, 350 kemil, 1kV  | 15         | 1.46E-03               | 5.22E-05             | 570                |

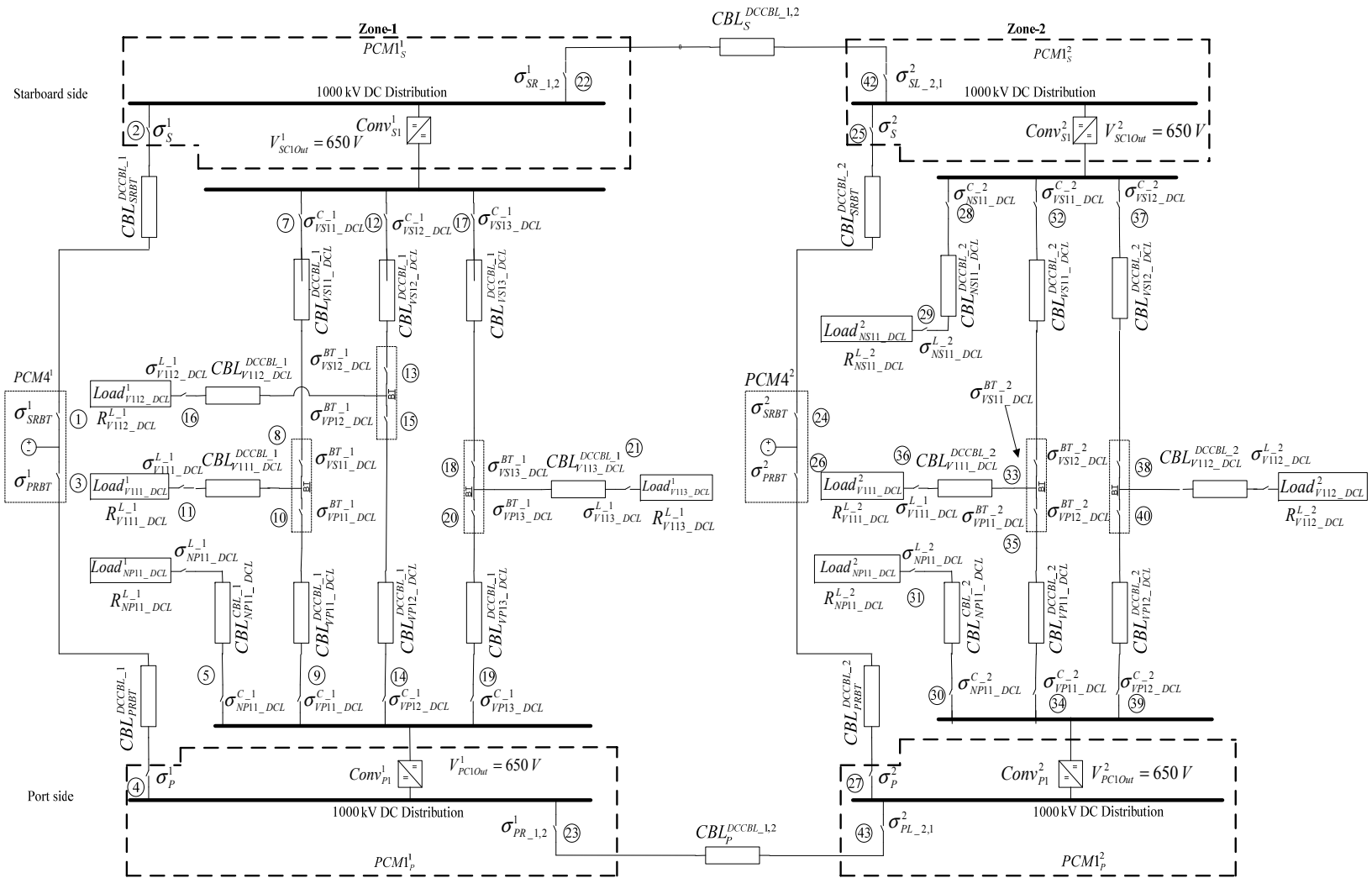


Fig. 5.2. Problem implementation: example power system

### **5.3. Failure Assessment Module and Pre/Post-Fault Information Extractor Module**

For the stable operation of SPS, it is imperative that the damage control method not select a faulted section of the SPS to re-energize during restoration. Hence, a failure assessment method that performs two functions, fault detection and fault location, is needed. The fault detection method detects an abnormal condition in the power system and determines whether there are any faults in the SPS. In case faults are detected, the fault location method locates the faulted components in the SPS. Previous work in PSAL [30] has developed such a method, but it was not integrated into this damage control method. Therefore, a stub routine, which contains user information providing fault information for a case study/scenario, was developed.

The pre/post-fault information extractor module was developed in visual C++. This module computes pre/post-fault data, such as pre-fault branch currents, pre-fault node voltages, and pre/post-fault switch status based on power system measurement stored in a text file during the power system simulation. In addition, the module determines the switches based on the faulted components, which if closed, can re-energize the faulted sections during restoration. The list of faulted components is provided as an input to the pre/post-fault information extractor module.

### **5.4. Case Studies**

To illustrate various aspects, such as load restoration and load shedding, of the genetic algorithm-based damage control solution, case studies were conducted. The

results of these simulations were designated in two possible solution categories: optimal and non-optimal solutions. A solution is considered optimal if the solution is able to restore all of the de-energized loads that are possible to be restored based on the priority of the load without violating the system operating constraints. A non-optimal solution is a solution that does not restore all of the de-energized loads that are possible to be restored. This thesis presents two case studies, which illustrate the damage control and load-shedding functions of the damage control method.

#### 5.4.1. Case Study 1

Case study 1 presents a multiple fault scenario at the cables supplying power to the DC vital loads, which have an alternate path. The purpose of this study is to illustrate the restorative operation of the damage control method.

##### 5.4.1.1. Initial Conditions

The system was considered to be working in starboard/port topology and had no constraint violations. The zone-1 PCM-4 and zone-3 PCM-4 were connected to the starboard side and port side buses, respectively. All loads were working, and the two zones were connected at starboard and port bus level. Each of the PCM-4 power capacities was considered to be 1100 kW. Table 5.3 presents the initial network configuration and provides a switch number for each switch in the solution provided by the damage control method. In Fig. 5.2, the encircled number next to each switch

represents the switch number. For example, the 3<sup>rd</sup> gene in the chromosome represents the switch status for the switch number-3 in Fig. 5.2.

#### 5.4.1.2. Fault Scenario

In this case study, a multiple fault scenario was considered, with faults in zone-1 at DC cables DCCBL\_1\_VS13\_DCL and DCCBL\_1\_VP12\_DCL. The result of this scenario was that the protective relays operated and opened the switches  $\sigma_{VS13\_DCL}^{C.1}$  and  $\sigma_{VP12\_DCL}^{C.1}$  upstream of the faults. These protective devices operation led to loss of supply to the two vital loads,  $Load_{V113\_DCL}^1$  and  $Load_{V112\_DCL}^1$ . The bold numbers in the post-fault configuration indicate the change in status for the corresponding switch from the pre-fault configuration.

#### 5.4.1.3. Simulation Results

Ten simulations were conducted for the above-mentioned scenario. In all of the simulations, optimal switch configurations were achieved. The supply to the de-energized vital loads ( $Load_{V112\_DCL}^1$  and  $Load_{V113\_DCL}^1$ ) were restored for the optimal solutions. The optimal solution achieved this through closing of switches  $\sigma_{VS12\_DCL}^{BT.1}$ ,  $\sigma_{VS12\_DCL}^{C.1}$ ,  $\sigma_{VP13\_DCL}^{C.1}$ , and  $\sigma_{VP13\_DCL}^{BT.1}$  and opening of switches  $\sigma_{VP12\_DCL}^{BT.1}$  and  $\sigma_{VS13\_DCL}^{BT.1}$ . Table 5.3 presents the details of simulations, objective function value, target value, error, solution category, and best chromosome achieved. The target value is the theoretically

computed objective function value for a given individual. The bold numbers in the best chromosome achieve indicate the change in status for the corresponding switch from the post-fault configuration. The error (%) value was calculated as:

$$Error(\%) = \frac{(Obj.func. value - Target value)}{Target value} * 100\% \tag{5.1}$$

Table 5.3. Results of case study 1

| Initial network configuration  |                  |              |          |                   | 1100111100100111110011100111111110010011111           |
|--|------------------|--------------|----------|-------------------|---|
| Configuration after protective devices action (post-fault configuration) |                  |              |          |                   | 11001111001000 <b>110</b> 100111001111111110010011111 |
| Switch sequence  |                  |              |          |                   | 1 2 3 .....41 42 43                                   |
| Simulation   | Obj. func. value | Target value | Error(%) | Solution category | Network configurations                                |
| 1  | 122.19           | 120          | 1.83     | Optimal           | 11001111001 <b>110010011</b> 111001111111110010011111 |
| 2  | 122.19           | 120          | 1.83     | Optimal           | 11001111001 <b>110010011</b> 111001111111110010011111 |
| 3  | 122.19           | 120          | 1.83     | Optimal           | 11001111001 <b>110010011</b> 111001111111110010011111 |
| 4  | 122.19           | 120          | 1.83     | Optimal           | 11001111001 <b>110010011</b> 111001111111110010011111 |
| 5  | 122.19           | 120          | 1.83     | Optimal           | 11001111001 <b>110010011</b> 111001111111110010011111 |
| 6  | 122.19           | 120          | 1.83     | Optimal           | 11001111001 <b>110010011</b> 111001111111110010011111 |
| 7  | 122.19           | 120          | 1.83     | Optimal           | 11001111001 <b>110010011</b> 111001111111110010011111 |
| 8  | 122.19           | 120          | 1.83     | Optimal           | 11001111001 <b>110010011</b> 111001111111110010011111 |
| 9  | 122.19           | 120          | 1.83     | Optimal           | 11001111001 <b>110010011</b> 111001111111110010011111 |
| 10   | 122.19           | 120          | 1.83     | Optimal           | 11001111001 <b>110010011</b> 111001111111110010011111 |

5.4.2. Case Study 2

Case study 2 presents a single fault scenario at the cable supplying power to a vital load in zone-2. The purpose of case study 2 is to illustrate the load-shedding function of the method. Zone-1 and zone-2 PCM-4 power capacity were considered as 500 kW and 1200 kW, respectively.

#### 5.4.2.1. Initial Conditions

The system was considered to be working in starboard/port side topology and had no constraint violations. The zone-1 PCM-4 was connected to the starboard side bus and the zone-2 PCM-4 was connected to the port side bus. The non-vital load  $Load_{NP11\_DCL}^2$  and the vital load  $Load_{V111\_DCL}^1$  were considered de-energized. The remaining loads either get power supply through the starboard or port side bus. The initial configuration is presented in Table 5.4.

#### 5.4.2.2. Fault Scenario

In case study 2, a single fault scenario was considered, with faults at DC cable DCCBL\_2\_VS11\_DCL. The result of this scenario was that the protective relay operated and opened the switch  $\sigma_{VS11\_DCL}^{C,2}$ . The protective device operation led to loss of supply to the vital load  $Load_{V111\_DCL}^2$ .

#### 5.4.2.3. Simulation Results

Ten simulations were conducted for the above-mentioned scenario. In most simulations, optimal switch configurations were achieved. The optimal solutions led to the restoration of vital load  $Load_{V111\_DCL}^2$  by transferring it to port side bus by opening switch  $\sigma_{VS11\_DCL}^{BT,2}$  and closing switches  $\sigma_{VP11\_DCL}^{C,2}$  and  $\sigma_{VP11\_DCL}^{BT,2}$ . In this, process a non-vital load  $Load_{NP11\_DCL}^1$  is shed by opening switch  $\sigma_{NP11\_DCL}^{L,1}$  to remove power capacity

violation caused by transfer of the vital load to the port side bus. In a few simulations, non-optimal solutions were achieved where the final network configuration achieved was the same as the post-fault configuration. Table 5.4 presents the details of the various simulations conducted for case study 2.

Table 5.4. Results of case study 2

| Initial network configuration  |                  |                |           |                   | 1100111100100111110011100111111110010011111 |
|--|------------------|----------------|-----------|-------------------|---|
| Configuration after protective devices action (post-fault configuration) |                  |                |           |                   | 1100111100100011010011100111111110010011111 |
| Switch sequence  |                  |                |           |                   | 1 2 3 .....41 42 43                         |
| Simulation   | Obj. func. Value | Expected value | Error (%) | Solution category | Network configurations                      |
| 1  | 122.54           | 120            | 2.12      | Optimal           | 1100111100111001001111100111111110010011111 |
| 2  | 122.54           | 120            | 2.12      | Optimal           | 1100111100111001001111100111111110010011111 |
| 3  | 122.54           | 120            | 2.12      | Optimal           | 1100111100111001001111100111111110010011111 |
| 4  | 492.42           | 490            | 0.49      | Non-optimal       | 0111111100111001001111111011111110010011111 |
| 5  | 492.42           | 490            | 0.49      | Non-optimal       | 0111111100111001001111111011111110010011111 |
| 6  | 122.54           | 120            | 2.12      | Optimal           | 1100111100111001001111100111111110010011111 |
| 7  | 122.54           | 120            | 2.12      | Optimal           | 1100111100111001001111100111111110010011111 |
| 8  | 122.54           | 120            | 2.12      | Optimal           | 1100111100111001001111100111111110010011111 |
| 9  | 122.54           | 120            | 2.12      | Optimal           | 1100111100111001001111100111111110010011111 |
| 10   | 122.54           | 120            | 2.12      | Optimal           | 1100111100111001001111100111111110010011111 |

#### 5.4.3. Case Study 3

Case study 3 presents a single fault scenario at the cable supplying power to one of the DC vital loads in zone-1. The purpose of this study is to check, whether algorithm is able to switch de-energized vital load to the alternate supply path, without affecting other loads in the system significantly.

#### 5.4.3.1. Initial Conditions

The system is working in normal state and has no system constraint violations. Zone-1 PCM-4 is connected to the starboard side bus and zone-2 PCM-4 is connected to the port side bus. All loads are energized and the two zones are connected to each other. Each PCM-4 power capacities considered is 1100 kW. The initial network configuration and a switch number sequence for network configuration is presented in Table 5.5.

#### 5.4.3.2. Fault Scenario

In this case study, a single fault scenario is considered, with fault at DC cable DCCBL\_1\_VS13\_DCL in zone-1. The result of this scenario is that the protective relays operate and open the switch  $\sigma_{VS13_1}^{C.1}$  upstream of the fault. This leads to loss of supply to the vital load  $Load_{V113\_DCL}^1$ .

#### 5.4.3.3. Simulation Results

Ten continuous simulations conducted for the above mentioned scenario. In all of the cases optimal switch configurations were achieved. The supply to the de-energized vital load  $Load_{V113\_DCL}^1$  was restored. The vital load  $Load_{V113\_DCL}^1$  and  $Load_{V112\_DCL}^2$  gets transferred to the port side bus and starboard side bus, respectively. This happens through the closing of switches  $\sigma_{VP13_1}^{C.1}$ ,  $\sigma_{VP13_1}^{BT.1}$ ,  $\sigma_{VS12\_DCL}^{C.2}$ , and  $\sigma_{VS12\_DCL}^{BT.2}$  and opening

of switch  $\sigma_{VS13\_1}^{BT\_1}$ , and  $\sigma_{VP12\_DCL}^{BT\_2}$  in case of optimal solution. The details of the various simulations are presented in Table 5.5.

Table 5.5. Results of case study 3

| Initial network configuration  |                  |                |           |                   | 1100111100100111110011100111111110010011111                   |
|--|------------------|----------------|-----------|-------------------|---|
| Configuration after protective devices action (post-fault configuration) |                  |                |           |                   | 11001111001001110100111001111111110010011111                  |
| Switch sequence  |                  |                |           |                   | 1 2 3 .....41 42 43   |
| Simulation   | Obj. func. value | Expected value | Error (%) | Solution category | Network configurations  |
| 1  | 122.56           | 120            | 2.13      | Optimal           | 110011110010011100 <b>11</b> 1110011111111001 <b>1110</b> 111 |
| 2  | 122.56           | 120            | 2.13      | Optimal           | 110011110010011100 <b>11</b> 1110011111111001 <b>1110</b> 111 |
| 3  | 122.56           | 120            | 2.13      | Optimal           | 110011110010011100 <b>11</b> 1110011111111001 <b>1110</b> 111 |
| 4  | 122.56           | 120            | 2.13      | Optimal           | 110011110010011100 <b>11</b> 1110011111111001 <b>1110</b> 111 |
| 5  | 122.56           | 120            | 2.13      | Optimal           | 110011110010011100 <b>11</b> 1110011111111001 <b>1110</b> 111 |
| 6  | 122.56           | 120            | 2.13      | Optimal           | 110011110010011100 <b>11</b> 1110011111111001 <b>1110</b> 111 |
| 7  | 122.56           | 120            | 2.13      | Optimal           | 110011110010011100 <b>11</b> 1110011111111001 <b>1110</b> 111 |
| 8  | 122.56           | 120            | 2.13      | Optimal           | 110011110010011100 <b>11</b> 1110011111111001 <b>1110</b> 111 |
| 9  | 122.56           | 120            | 2.13      | Optimal           | 110011110010011100 <b>11</b> 1110011111111001 <b>1110</b> 111 |
| 10   | 122.56           | 120            | 2.13      | Optimal           | 110011110010011100 <b>11</b> 1110011111111001 <b>1110</b> 111 |

#### 5.4.4. Case Study 4

This case study presents a single fault scenario at one of the tie cables connecting two DC zones, which results in more than one load getting de-energized. The purpose of this study is to check, whether algorithm is able to restore all the loads back to the normal state without violating any constraint.

#### 5.4.4.1. Initial Conditions

The system is in normal state and no system constraints are violated. Zone-1 PCM-4 is connected to the starboard side bus and zone-2 PCM-4 is connected to the port side bus. All loads are energized and the two zones are connected to each other. Each PCM-4 power capacities considered is 1100 kW. The initial network configuration and a switch number sequence for network configuration is presented in Table 5.6.

#### 5.4.4.2. Fault Scenario

A single fault at DC tie cable DCCBL\_12\_P is considered. The result of this scenario is that the protection relay operates and opens switches  $\sigma_{PR_{12}}^1$  and  $\sigma_{PL_{21}}^2$ . This leads to isolation of zone-1 port bus and supply is lost to the vital load  $Load_{V112\_DCL}^1$  and the non-vital load  $Load_{NP11\_DCL}^1$ .

#### 5.4.4.3. Simulation Results

Ten simulation studies were conducted with the above mentioned scenario. In most of the cases optimal switch configurations were achieved. In this scenario, considering the entire possible switch configuration, at least one of the loads will lose power supply. As the ratings of non-vital loads  $Load_{NP11\_DCL}^1$  and  $Load_{NS11\_DCL}^2$  are of same size, the weights obtained for these two loads are same. Therefore, the optimal switch configuration results in non-vital load  $Load_{NP11\_DCL}^1$  not getting restored. The

system goes for keeping the other non-vital load  $Load_{NS11\_DCL}^2$  still energized, as number of switching actions required are much less as compared to the restoring non-vital load  $Load_{NP11\_DCL}^1$ . In one of the simulations a non-vital solution was obtained where a vital load was not restored. All the vital loads in zone - 1 are also transferred to the port bus. The non-optimal solution results to de-energization of non-vital load  $Load_{NS11\_DCL}^2$ . The details of the various simulations are presented in Table 5.6. In two simulations non-optimal solutions were obtained, where method was not able to restore one or more loads.

Table 5.6. Results of case study 4

| Initial network configuration  |                  |                |           |                   | 110011110010011111001110011111110010011111  |
|--|------------------|----------------|-----------|-------------------|---|
| Configuration after protective devices action (post-fault configuration) |                  |                |           |                   | 110011110010011111001100011111110010011110  |
| Switch sequence  |                  |                |           |                   | 1 2 3 .....41 42 43                         |
| Simulation   | Obj. func. value | Expected value | Error (%) | Solution category | Network configurations                      |
| 1  | 1158.1           | 1157.06        | 0.09      | Non-optimal       | 1100111100111101110011000110111110010011110 |
| 2  | 659.97           | 658.46         | 0.23      | Optimal           | 1100111100111101110011000111111101110011110 |
| 3  | 659.97           | 658.46         | 0.23      | Optimal           | 1100111100111101110011000111111101110011110 |
| 4  | 1158.1           | 1157.06        | 0.09      | Non-optimal       | 1100111100111101110011000110111110010011110 |
| 5  | 659.97           | 658.46         | 0.23      | Optimal           | 1100111100111101110011000111111101110011110 |
| 6  | 659.97           | 658.46         | 0.23      | Optimal           | 1100111100111101110011000111111101110011110 |
| 7  | 659.97           | 658.46         | 0.23      | Optimal           | 1100111100111101110011000111111101110011110 |
| 8  | 659.97           | 658.46         | 0.23      | Optimal           | 1100111100111101110011000111111101110011110 |
| 9  | 659.97           | 658.46         | 0.23      | Optimal           | 1100111100111101110011000111111101110011110 |
| 10   | 659.97           | 658.46         | 0.23      | Optimal           | 1100111100111101110011000111111101110011110 |

#### 5.4.5. Case Study 5

This case study presents a single fault scenario (similar to case study 1) at one of the cables supplying power DC vital load, with an alternate possible path of supply. The

only difference between case study 1 and this case study is that one of the non-vital loads is considered switched off. The purpose of this study is to check, whether algorithm is able to switch de-energized vital load to the alternate supply path, and should not turn on the switched off non-vital load.

#### 5.4.5.1. Initial Conditions

The system is in normal state and no system constraints are violated. Zone-1 PCM-4 is connected to the starboard side bus and zone-2 PCM-4 is connected to the port side bus. All loads are energized except non-vital load  $Load_{NP11\_DCL}^1$  and the two zones are connected to each other. Each PCM-4 power capacities considered is 1100 kW. The initial network configuration and a switch number sequence for network configuration is presented in Table 5.7.

#### 5.4.5.2. Fault Scenario

A single fault in zone – 1 DC cable DCCBL\_1\_VS13\_DCL is considered. The result of this scenario is that the line protection relay opens the switch  $\sigma_{VS13\_1}^{C-1}$  upstream of the fault. This leads to loss of supply to the vital load  $Load_{V113\_DCL}^1$ .

### 5.4.5.3. Simulation Results

Ten simulation studies were conducted with the above mentioned scenario. In all simulations optimal switch configurations were reached. As a result of the optimal configurations, the supply to the de-energized vital load  $Load_{V113\_DCL}^1$  was restored, without affecting other loads. The vital load  $Load_{V113\_DCL}^1$  gets transferred to the port bus. This happens through the closing of switches  $\sigma_{VP13\_1}^{C\_1}$  and  $\sigma_{VP13\_1}^{BT\_1}$  and opening of switch  $\sigma_{VS13\_1}^{BT\_1}$ , in case of optimal solution. The details of the various simulations are presented in Table 5.7.

Table 5.7. Results of case study 5

| Initial network configuration  |                  |                |           |                   | 1100001100100111110011100111111110010011111           |
|--|------------------|----------------|-----------|-------------------|---|
| Configuration after protective devices action (post-fault configuration) |                  |                |           |                   | 11000011001001110100111001111111110010011111          |
| Switch sequence  |                  |                |           |                   | 1 2 3 .....41 42 43                                   |
| Simulation   | Obj. func. value | Expected value | Error (%) | Solution category | Network configurations                                |
| 1  | 61.76            | 60             | 2.93      | Optimal           | 110000110010011100 <b>11</b> 111001111111110010011111 |
| 2  | 61.76            | 60             | 2.93      | Optimal           | 110000110010011100 <b>11</b> 111001111111110010011111 |
| 3  | 61.76            | 60             | 2.93      | Optimal           | 110000110010011100 <b>11</b> 111001111111110010011111 |
| 4  | 61.76            | 60             | 2.93      | Optimal           | 110000110010011100 <b>11</b> 111001111111110010011111 |
| 5  | 61.76            | 60             | 2.93      | Optimal           | 110000110010011100 <b>11</b> 111001111111110010011111 |
| 6  | 61.76            | 60             | 2.93      | Optimal           | 110000110010011100 <b>11</b> 111001111111110010011111 |
| 7  | 61.76            | 60             | 2.93      | Optimal           | 110000110010011100 <b>11</b> 111001111111110010011111 |
| 8  | 61.76            | 60             | 2.93      | Optimal           | 110000110010011100 <b>11</b> 111001111111110010011111 |
| 9  | 61.76            | 60             | 2.93      | Optimal           | 110000110010011100 <b>11</b> 111001111111110010011111 |
| 10   | 61.76            | 60             | 2.93      | Optimal           | 110000110010011100 <b>11</b> 111001111111110010011111 |

### 5.4.6. Case Study 6

This case study presents a single fault scenario at the vital DC load cable, resulting in a post-fault switch configuration/system, which cannot be further improved.

That means the post-fault configuration itself is the optimal solution. The purpose of this case study is to check, if the configuration reached by the method is same as that of post-fault configuration or not.

#### 5.4.6.1. Initial Conditions

The system is normal state and no system constraints are violated. Zone-1 PCM-4 is connected to the starboard side bus and zone-2 PCM-4 is connected to the port side bus. All loads are energized and the two zones are connected to each other. Each PCM-4 has capacity of 1100 kW. The initial network configuration and a switch number sequence for network configuration is presented in Table 5.8.

#### 5.4.6.2. Fault Scenario

A single fault in zone – 1 DC cable DCCBL\_1\_V113\_DCL is considered. As a result of this the line protection relay opens the switch  $\sigma_{V_{S13_1}}^{C,1}$  upstream of the fault. This leads to loss of supply to the vital load  $Load_{V_{113\_DCL}}^1$ .

#### 5.4.6.3. Simulation Results

Ten simulation studies were conducted with the above mentioned scenario. In all simulations optimal switch configurations were reached, which is same as the post-fault configuration. The details of the various simulations are presented in Table 5.8. In this

simulation no switching actions were suggested by the genetic algorithm. The final network configuration achieved was exactly same as the post-fault configuration.

Table 5.8. Results of case study 6

| Initial network configuration  |                  |                |           |                   | 110011110010011111001110011111110010011111 |
|--|------------------|----------------|-----------|-------------------|--|
| Configuration after protective devices action (post-fault configuration) |                  |                |           |                   | 110011110010011101001110011111110010011111 |
| Switch sequence  |                  |                |           |                   | 1 2 3 .....41 42 43                        |
| Simulation   | Obj. func. value | Expected value | Error (%) | Solution category | Final network configuration                |
| 1  | 808.94           | 807.69         | 0.15      | Optimal           | 110011110010011101001110011111110010011111 |
| 2  | 808.94           | 807.69         | 0.15      | Optimal           | 110011110010011101001110011111110010011111 |
| 3  | 808.94           | 807.69         | 0.15      | Optimal           | 110011110010011101001110011111110010011111 |
| 4  | 808.94           | 807.69         | 0.15      | Optimal           | 110011110010011101001110011111110010011111 |
| 5  | 808.94           | 807.69         | 0.15      | Optimal           | 110011110010011101001110011111110010011111 |
| 6  | 808.94           | 807.69         | 0.15      | Optimal           | 110011110010011101001110011111110010011111 |
| 7  | 808.94           | 807.69         | 0.15      | Optimal           | 110011110010011101001110011111110010011111 |
| 8  | 808.94           | 807.69         | 0.15      | Optimal           | 110011110010011101001110011111110010011111 |
| 9  | 808.94           | 807.69         | 0.15      | Optimal           | 110011110010011101001110011111110010011111 |
| 10   | 808.94           | 807.69         | 0.15      | Optimal           | 110011110010011101001110011111110010011111 |

### 5.5. Summary of Results

In most cases, the damage control algorithm was able to restore the system without violating the system operating. In only four out of sixty simulations conducted over six different case studies, the solutions obtained were non-optimal. These non-optimal solutions were observed in simulations for case study 2 and case study 4. The reason for the non-optimal solutions observed in case study 4 can be ascribed to increase in the size of infeasible region, because of more number of switches which should not be closed, as compared to other case studies. In case study 2, two non-optimal solutions were observed. The reason for the two non-optimal solution case study 2 not certain and

needs more work to make any generalized statement. The overall result for the simulations conducted is shown in Fig. 5.3.

The objective function values achieved were slightly different from the target values. This error in the objective function value was because of the inconsistencies in the cable and PCM-1 models between PSCAD and IDA. The cables were modeled as the RLC lumped parameter pi-section model in PSCAD, while only line resistance and self-inductance were modeled in the cable model in the DAE equations in IDA. The second source of error was in the model of PCM-1. The DC-DC converter was modeled with closed loop control in PSCAD, while it was modeled as a DC-DC transformer in the DAEs in IDA. A maximum error of 2.93% was observed throughout all the case studies conducted.

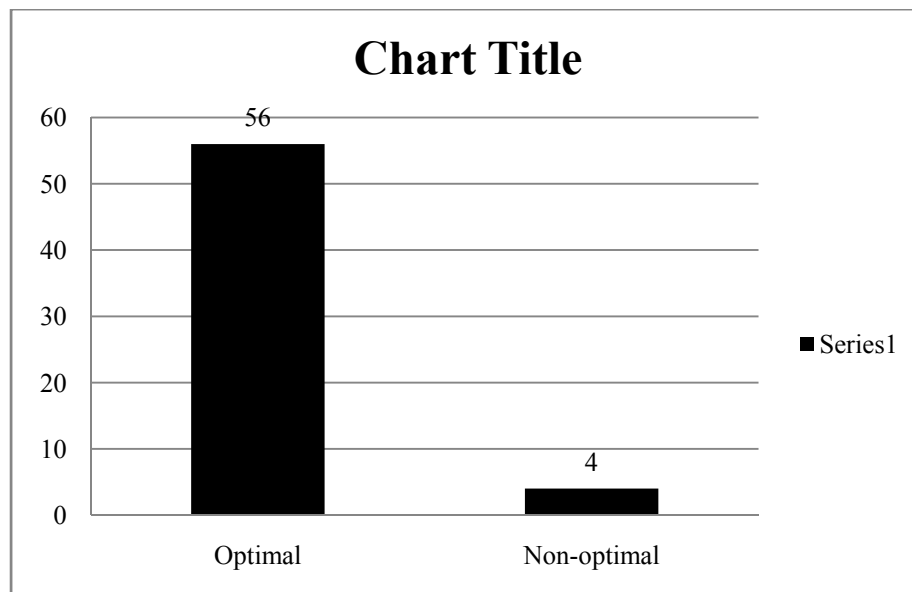


Fig. 5.3. Overall results of solution category

## **5.6. Summary**

The Section 5 provided details of various case studies conducted to test the effectiveness of the new static genetic algorithm-based damage control method.

## 6. CONCLUSION

### 6.1. Overview of Research Work

The research work presented in the thesis is a part of overall research project being conducted by Power System Automation Laboratory (PSAL). The overall objective of the research work conducted at PSAL was to develop a damage control solution for next generation SPS at two levels: IPS HV/MV AC level, and DC zonal IFTP system. This thesis presented a static implementation of a new damage control method for a notional next generation integrated power system at DC zonal IFTP system based on a dynamic formulation. The static damage control problem was implemented as a constrained optimization problem with system operating limits as constraints. The damage control algorithm developed used constrained binary genetic algorithm to search the optimal network configuration, which restores the power system without violating the system constraints. Though, the dynamic problem formulation included DAEs as the constraints, the static implementation used DAEs for the computation of power system variables for objective function computation and operating limits checking only. A few off-line studies were conducted using an example power system modeled in PSCAD to evaluate the effectiveness of the static damage control method.

## 6.2. Conclusions

Based on studies conducted for the example power system developed, various observations were made:

- a) In most simulations conducted on various case studies, optimal network configurations were achieved. The optimal solution produced reliable restoration of system. In few simulations, the results obtained were not optimal, meaning that the power system was not fully restored.
- b) In scenarios where the infeasible region, in the solution space, was bigger, more number of non-optimal solutions was obtained than in scenarios, where the infeasible region was smaller.
- c) Better convergence was observed with repair probability of 10%. With higher or lower repair-and-replace probability the more number of non-optimal solutions were obtained.
- d) It was observed that the heuristic rules (used in repair function, and in defining feasibility of an individual) helped the damage control method to search through the solution space for the optimal solutions. In absence of the heuristic rules the convergence rate of the proposed method was reduced.

## 6.3. Future Work

Future research work for the proposed dynamic damage control method involves developing a dynamic implementation of the damage control method, improving its

efficiency by fine-tuning the genetic algorithm method parameters, and improving or adding heuristic rules used as repair functions. In addition, DAEs for PCM-1, PCM-2, and PCM-4 will be included in the next DC zonal IFTP model. A similar problem formulation for notional next generation SPS HV/MV IPS will also be implemented.

## REFERENCES

- [1] C. Dafis, "Development of a power system management tool to support automated damage control for shipboard power system", [Online]. Available: [http://www.navysbir.com/n06\\_3/navysb063-177.htm](http://www.navysbir.com/n06_3/navysb063-177.htm). [Accessed: Nov. 5, 2007]
- [2] D. S. Parker and C. G. Hodge, "The electric warship," in *Proc. 8<sup>th</sup> International Conference on Electrical Machines and Drives*, Cambridge, UK, Sept. 1-3, 1997, pp. 319-325.
- [3] S. Srivastava and K. L. Butler-Burry, "Expert-system method for automatic reconfiguration for restoration of shipboard power systems," *IEE Proceedings - Generation, Transmission and Distribution*, vol. 153, pp. 253-260, 2006.
- [4] K. L. Butler-Purry, N. D. R. Sarma, and I. V. Hicks, "Service restoration in naval shipboard power systems," *IEE Proceedings - Generation, Transmission and Distribution*, vol. 151, pp. 95-102, 2004.
- [5] N. Doerry, H. Robey, J. Amy, and C. Petry, "Powering the future with the integrated power system," *Naval Engineers Journal*, vol. 108, pp. 267-282, 1996.
- [6] B. R. Williams, D. G. Walden, and S. C. E. Co, "Distribution automation strategy for the future-changing the momentum," *Computer Applications in Power, IEEE*, vol. 7, pp. 16-21, 1994.
- [7] S. Khushalani and N. N. Schulz, "Restoration optimization with distributed generation considering islanding," in *Proc. IEEE Power Engineering Society General Meeting*, San Francisco, CA, June 12-16, 2005, pp. 743-747.
- [8] K. L. Butler, N. D. R. Sarma, and V. Ragendra Prasad, "Network reconfiguration for service restoration in shipboard power distribution systems," *IEEE Trans. Power Systems*, vol. 16, pp. 653-661, 2001.
- [9] M. M. Adibi, L. R. J. Kafka, and D. P. Milanicz, "Expert system requirements for power system restoration," *IEEE Trans. Power Systems*, vol. 9, pp. 1592-1600, 1994.
- [10] Y. Y. Hsu and H. C. Kuo, "A heuristic based fuzzy reasoning approach for distribution system service restoration," *IEEE Trans. Power Delivery*, vol. 9, pp. 948-953, 1994.

- [11] Y. Y. Hsu and H. M. Huang, "Distribution system service restoration using the artificial neural network approach and pattern recognition method," *IEE Proceedings - Generation, Transmission and Distribution*, vol. 142, pp. 251-256, 1995.
- [12] H. Kim, Y. Ko, and K. H. Jung, "Artificial neural-network based feeder reconfiguration for loss reduction in distribution systems," *IEEE Trans. Power Delivery*, vol. 8, pp. 1356-1366, 1993.
- [13] N. Kumar, A. K. Srivastava, and N. N. Schulz, "Shipboard power system restoration using binary particle swarm optimization," in *Proc. 39<sup>th</sup> North American Power Symposium*, Las Cruces, NM, Sept. 30 - Oct. 2, 2007, pp. 164-169.
- [14] J. A. Momoh, Y. Xia, and K. C. Alfred, "Dynamic reconfiguration for shipboard power system using multi-agent system," in *Proc. IEEE Power and Energy Society General Meeting-Conversion and Delivery of Electrical Energy in the 21st Century*, Pittsburgh, PA, July 9-13, 2008, pp. 1-4.
- [15] K. Davey, R. Longoria, W. Shutt, J. Carroll, K. Nagaraj, J. Park, T. Rosenwinkel, W. Wu, and A. Arapostathis, "Reconfiguration in shipboard power systems," in *Proc. American Control Conference*, New York, NY, July 9-13, 2007, pp. 4750-4755.
- [16] H. G. Kwatny, E. Mensah, D. Niebur, and C. Teolis, "Optimal shipboard power system management via mixed integer dynamic programming," in *Proc. Electric Ship Technologies Symposium*, Philadelphia, PA, July 25-27, 2005, pp. 55-62.
- [17] J. Inagaki, J. Nakajima, and M. Haseyama, "A multi-objective service restoration method for power distribution systems," in *Proc. IEEE International Symposium on Circuits and Systems*, Kos, Greece, May 21-24, 2006, pp. 1784-1787.
- [18] K. Manjunath and M. R. Mohan, "A new hybrid multi-objective quick service restoration technique for electric power distribution systems," *International Journal of Electrical Power and Energy Systems*, vol. 29, pp. 51-64, 2007.
- [19] C. R. Reeves and J. E. Rowe, *Genetic Algorithms-Principles and Perspectives: A Guide to GA Theory*, 1st ed. Boston: Kluwer Academic Publishers, 2003.
- [20] K. R. Padamati, N. N. Schulz, and A. K. Srivastava, "Application of genetic algorithm for reconfiguration of shipboard power system," in *Proc. 39<sup>th</sup> North American Power Symposium*, Las Cruces, NM, Sept. 30 - Oct. 2, 2007, pp. 159-163.

- [21] Q. Zhou, D. Shirmohammadi, W. H. E. Liu, and C. A. San Francisco, "Distribution feeder reconfiguration for service restoration and load balancing," *IEEE Trans. Power Systems*, vol. 12, pp. 724-729, 1997.
- [22] X. Yang and Y. Zhang, "Intelligent real-time fault restoration of the large shipboard power system based on genetic algorithm," *International Journal of Information Technology*, vol. 11, 2005.
- [23] R. L. Haupt and S. E. Haupt, *Practical Genetic Algorithms*, 2nd ed. Hoboken, NJ: Wiley-Interscience Publication, 1998.
- [24] H. Pohlheim, "GEATbx: Genetic and Evolutionary Algorithm Toolbox for use with MATLAB Documentation", Dec. 2006, [Online]. Available: <http://geatbx.com/docu/index.html>. [Accessed: Jan. 3, 2008]
- [25] "Genetic algorithm", [Online]. Available: [http://en.wikipedia.org/wiki/Genetic\\_algorithm](http://en.wikipedia.org/wiki/Genetic_algorithm). [Accessed: Sept. 10, 2007]
- [26] H. Pohlheim, "GEATbx - The Genetic and Evolutionary Algorithm Toolbox for Matlab", [Online]. Available: <http://geatbx.com/>. [Accessed: Jan. 3, 2008]
- [27] D. Orvosh and L. Davis, "Using a genetic algorithm to optimize problems with feasibility constraints," in *Proc. IEEE Conference on Evolutionary Computation*, Orlando, FL, Jun 27-29, 1994, pp. 548-553.
- [28] A. E. Smith and D. W. Coit, "Penalty functions," in *Handbook of Evolutionary Computation*, 1st ed, T. Baeck, D. Fogel, and Z. Michalewicz, Eds.: A Joint Publication of Oxford University Press and Institute of Physics Publishing, Sept. 1995.
- [29] A. C. Hindmarsh, P. N. Brown, K. E. Grant, S. L. Lee, R. Serban, D. E. Shumaker, and C. S. Woodward, "SUNDIALS: Suite of nonlinear and differential/algebraic equation solvers," *ACM Trans. Mathematical Software*, vol. 31, pp. 363-396, 2005.
- [30] S. K. Srivastava, K. L. Butler-Purry, and N. D. R. Sarma, "Shipboard power restored for active duty," *IEEE Computer Applications in Power*, vol. 15, pp. 16-23, 2002.

## VITA

Tushar Amba received his B.E. in electrical engineering in 2004, from Thapar Institute of Engineering and Technology, India. He joined Siemens Power Engineering Limited in India, where he worked as an electrical engineer from 2004 to 2006. He joined the master's program in electrical engineering at Texas A&M University, in 2006. He received his M.S. in electrical engineering in May 2009, from Texas A&M University. His research interests are in the area of distribution automation and intelligent systems for damage control on shipboard power systems.

Tushar can be reached by email at [tushar.amba@gmail.com](mailto:tushar.amba@gmail.com) or by mail at Department of Electrical and Computer Engineering, MS 3128, College Station, TX 77843.